# AEROELASTIC ANALYSIS OF ACTIVELY CONTROLLED SMART WIND TURBINE BLADES

BY

**HAMZA AHMED MIR**

A Thesis Presented to the

DEANSHIP OF GRADUATE STUDIES

**KING FAHD UNIVERSITY OF PETROLEUM & MINERALS**

DHAHRAN, SAUDI ARABIA

In Partial Fulfillment of the
Requirements for the Degree of

# MASTER OF SCIENCE

In

AEROSPACE ENGINEERING

**DECEMBER, 2017**

# KING FAHD UNIVERSITY OF PETROLEUM & MINERALS
## DHAHRAN 31261, SAUDI ARABIA

## DEANSHIP OF GRADUATE STUDIES

This thesis, written by **HAMZA AHMED MIR** under the direction of his thesis adviser and approved by his thesis committee, has been presented to and accepted by the Dean of Graduate Studies, in partial fulfillment of the requirements for the degree of **MASTER OF SCIENCE IN AEROSPACE ENGINEERING DEPARTMENT**.

**Thesis Committee**

_____
Dr. Wael G Abdelrahman (Adviser)

_____
Dr. Ahmed Z. Al-Garni (Co-adviser)

_____
Dr. Prasetyo Edi (Member)

_____
Dr. Yehia A. Khulief (Member)

_____
Dr. Salih O. Duffuaa (Member)

_____
Dr. Ayman M. Abdallah
Department Chairman

_____
Dr. Salam A. Zummo
Dean of Graduate Studies

3|5|18
_____
Date

*This dissertation is dedicated to my parents for their continuous support, encouragement, guidance and prayers throughout my professional and academic carrier. Also, to all my teachers and mentors, for their endeavours in providing me with an excellent conducive ambience through their supervision, enlightenment, expertise and relentless assistance.*

# ACKNOWLEDGMENTS

*First, I would like to thank Almighty Allah for bestowing me with cognitive abilities and helping me to complete this research work. Verily, all the praise is for Him and He alone possess the keys to all treasures of knowledge. Also, may Allah bestows His countless blessings upon His beloved Prophet Muhammad (S.A.W), his companions and on all rightly guided followers.*

I would like to express a deep sense of gratitude towards my mentor and adviser, Dr. G Wael Abdelrahman for his continuous support, counselling, dedication and encouragement throughout the duration of my thesis and overall stay at KFUPM. I would like to appreciate my co-advisor Dr. Ahmed Z. Al-Garni for providing me with an insight and profuse knowledge about aerodynamics of Wind Turbines. Also, I would especially like to acknowledge all the committee members, including Dr. Salih O. Duffuaa, Dr. Edi Prasetyo and Dr Yehia A. Khulief for their contribution towards all aspects of this dissertation particularly in portions relating to aeroelasticity and control techniques. I feel indebted for their overall support and their eagerness to provide me with very precious and fruitful information about my overall research. Moreover, I would like to appreciate Chairman of Aerospace Department Dr. M Ayman Abdallah, for his candid

support, kindness and also for providing me with an excellent opportunity to work in the department. His unremitting support really helped me to come through with flying colors. Also, I would like to express special gratitude to Dr. Steen Krenk, professor in Department of Mechanical Engineering at Technical University of Denmark for enriching me with precious resources along with in-depth information regarding my work.

Also, I would like to extend my gratitude towards my parents for their love and relentless prayers without which this work could never have been accomplished. To my brothers, for their encouragement and support in all walks of my life.

I would like to thank all the friends and the Pakistan Community for their social, financial and emotional support and imprinting delightful memories on my mind. I would especially like to mention my friends Muhammad Umar Azam from Pakistan and Shadi Ayman Alhaj from Jordon for supporting me during my tough times and making my stay at KFUPM a very pleasant one. I would especially like to applaud the support from my colleagues especially, Mr. Mohammed Abdul Muqeeth, Mr. Sultan M. Ghazzawi and Mr. Sherif Ibrahim. Finally, I would also like to acknowledge and express my gratitude towards the management, administration and staff members of KFUPM for making my stay enjoyable and providing me with an amazing learning ambience. It was a truly wonderful experience and an honour to study under some of the world best teachers.

# TABLE OF CONTENTS

# LIST OF TABLES

# LIST OF FIGURES

# LIST OF ABBREVIATIONS

$\acute{a}$          Angular induction factor

$\alpha$          Rotation along x-axis

$\alpha_0$          Angle of attack due to profile camber

$\alpha_D$          Angle of attack due to damping

$\alpha_f$          Mean inflow angle due to rigid blade profile

$\alpha_K$          Angle of attack due to blade deformation

$\alpha_r$          Relative angle of attack

$\alpha_U$          Mean wind flow angle

$\bar{L}^c, \bar{L}^s$          Influence coefficient matrices

$\beta$          Rotation along y-axis

$\beta_r$          Relative flow angle

$\beta_t$          Blade twist angle

$\dot{G}$          Gyroscopic angular acceleration matrix

$\gamma$          Torsional deformation along z-axis

| | |
|---|---|
| $\gamma_e$ | Mass flow matrix |
| $\hat{\omega}$ | Skew symmetric angular velocity matrix |
| $\hat{S}$ | Initial stress matrix |
| $\hat{T}$ | Transformation matrix for initial stress |
| $\lambda$ | Tip speed ratio |
| $\lambda_0$ | Induced flow |
| $\lambda_r$ | Local speed ratio |
| $\Omega$ | Rotational Velocity of Wind Turbine |
| $\omega_k$ | Reduced frequency |
| $\omega_w$ | Whirl angular velocity |
| $\phi_j^r$ | Expansion functions |
| $\Psi$ | Angle x-axis make with turbine blade |
| $\rho$ | density of material |
| $\sigma_S$ | Solidity |
| $\sigma_p$ | Piezoelectric stress matrix |
| $\tau_n^{mc}, \tau_n^{ms}$ | Forcing vectors for Peters-He model |
| $\theta$ | Rigid body rotation along z-axis |
| $\varepsilon_0$ | Dielectric permittivity |
| $\vec{\sigma_e}$ | Elastic Stress Vector |
| $\vec{\varepsilon_e}$ | Elastic Strain Vector |

$\vec{D_e}$        Electric displacement vector

$\vec{E_f}$        Electric field vector

$a$        Axial factor

$A^\rho$        Weighted Area

$A_B$        Area of Beam

$A_D$        Aerodynamic force matrix for damping

$A_K$        Aerodynamic force matrix for stiffness

$A_S$        Shear center

$a_x, a_y, a_z$        Shear center coordinates

$C$        Cross-section flexibility matrix

$C_e$        Elastic Matrix at constant electric field

$C_K$        Centrifugal stiffness matrix

$C_P$        Power coefficient

$C_T$        Thrust coefficient

$c_x, c_y, c_z$        Coordinates of elastic center position vector

$D$        Equivalent damping matrix

$D_a$        Aerodynamic damping matrix

$E$        Young Modulus

$f$        Equivalent force vector

$F_a$        Aerodynamic force matrix

| | |
|---|---|
| $f_a$ | Aerodynamic force vector |
| $f_C$ | Centrifugal force vector |
| $f_e$ | External force vector |
| $f_G$ | Angular acceleration force vector |
| $G_S$ | Shear modulus |
| $G_D$ | Skew symmetric gyroscopic coupling matrix |
| $HAWT$ | Horizontal Axis Wind Turbine |
| $I$ | Moment of Inertia |
| $I_{yy}^\rho$ | Moment of inertia about y-axis |
| $I_{zy}^\rho$ | Product of inertia |
| $I_{zz}^\rho$ | Moment of inertia about z-axis |
| $J_0$ | Bessel functions of the first kind |
| $K$ | Equivalent stiffness matrix |
| $K_a$ | Aerodynamic stiffness matrix |
| $K_e$ | Elastic stiffness matrix |
| $K_g$ | Geometric element stiffness matrix |
| $K_{cs}$ | Cross-section stiffness matrix |
| $L$ | Length of the beam |
| $L_f$ | Aerodynamic Lift force |
| $M$ | Equivalent mass matrix |

| | |
|---|---|
| $M_y, M_z$ | Section moments |
| $N_1^a,\ N_q^a,\ N_r^a,\ N_1^b,\ N_q^b,\ N_r^b$ | Shape Functions |
| $N_A$ | Area interpolation matrix |
| $N_x$ | Longitudinal interpolation matrix |
| $Q_x, Q_y, Q_z$ | Section forces |
| $R_a$ | Transformation matrix for rotation |
| $S$ | Stress matrix |
| $S^0$ | Stress integral for initial stress matrix $\hat{S}$ |
| $S_y^\rho$ | Section moment about y-axis |
| $S_z^\rho$ | Section moment about z-axis |
| $S_{ref}$ | Blade reference area |
| $T_a$ | Transformation matrix for forces & moments |
| $T_d$ | Distribution matrix |
| $T_e$ | Transformation matrix for internal forces to nodal forces |
| $T_m$ | Kinetic energy function |
| $T_c(x)$ | Centrifugal Tensile Load at a distance x from the axis of rotation |
| $U$ | Relative wind velocity |
| $u$ | Deformation along x-axis |
| $U_D$ | Flow speed parallel to the chord |
| $U_y, U_z$ | Components of relative wind velocity |

| | |
|---|---|
| $v$ | Deformation along y-axis |
| $V_m$ | Potential energy function |
| $V_n^m$ | mass flow matrix |
| $VAWT$ | Vertical Axis Wind Turbine |
| $w$ | Deformation along z-axis |
| $w_0, w_1$ | Fourier coefficients |
| $W_i$ | Weighing coefficient |

# THESIS ABSTRACT

| | |
|---|---|
| **NAME:** | Hamza Ahmed Mir |
| **TITLE OF STUDY:** | Aeroelastic Analysis of Actively Controlled Smart Wind Turbine Blades |
| **MAJOR FIELD:** | Aerospace Engineering |
| **DATE OF DEGREE:** | December, 2017 |

*Wind energy has established itself as an invaluable renewable source and a replacement for fossil fuels. The objective of this research is to present a more realistic aeroelastic model of wind turbine blade and the aerodynamic forces in order to actively control the Wind Turbine edge-wise vibrations in a more effective way by utilizing smart materials. The challenge faced by research community is to develop a realistic aeroelastic model as the control effectiveness depends on how closely the proposed model emulates the real time forces and conditions. The methodology adopted for the active control of Wind Turbines was mainly simulation based and focused on adopting an aeroelastic model for a rotating wind turbine blade. This proposed model is the modified aeroelastic model, initially known as Peters-He Model, which includes structural-dynamic model, induced flow model*

*along with the airloads model. The aerodynamics and airfoil effects are based on a ONERA type model and the integration of structural-dynamics with airloads allow this model to include the past history of blade motions. The technique also employed various approximate analytical methods such as FEM and Rayleigh-Ritz method to obtain stiffness and mass matrix. The Euler-Bernoulli beam equation was solved for the free and forced response after its conversion into State Space Matrix form to obtain mode shape and natural frequencies. The uniform cantilever beam was used as an initial point to validate MATLAB code for different analytical methods and the results from the MATLAB code were compared with those given in the literature. The results for stiffness and mass matrix were found to be comparable and the state space model was obtained which was used to develop a reliable vibration control mechanism using LQR control. The state space model was modified to account for piezoelectric patch attached to beam for vibration suppression. The results show improvement in edgewise vibration of a wind turbine model. The technique enhances the real control effectiveness and effectively incorporates forces and atmospheric conditions. The results depict improvement in controlling the edgewise vibration of a wind turbine blade.*

*Keywords: edge-wise vibrations, Aeroelastic model, Wind Turbines, LQR Control*

# ملخص الرسالة

**الاسم الكامل :** حمزه احمد ميرطيب نيثار احمد

**عنوان الرسالة :** تحليل المرونة الهوائية للشفرات الذكية لدوارات الرياح ذات التحكم النشط

**التخصص:** هندسة الطيران والفضاء

**تاريخ الدرجة العلمية  :**دسمبر ٢٠١٧

أثبتت طاقة الرياح نفسها كمصدر متجدد لا يقدر بثمن، وبديل للوقود الأحفوري. والهدف من هذاالبحث هو تقديم نموذج للمرونة الهوائية لشفرات دوارات الرياح وقوى الحركية الهوائية عليهابحيث يكون أكثر واقعية، وذلك من أجل التحكم بطريقة نشطة في الاهتزازات في اتجاه حافة شفرة الدوار بطريقة أكثر كفاءة من خلال استخدام المواد الذكية. يتمثل التحدي الذي يواجهه المجتمع البحثي في تطوير نموذج واقعي للمرونة الهوائية، حيث تعتمد كفاءة التحكم على مدى اقتراب النموذج المقترح من تمثيل القوى والظروف في الوقت الفعلي.إن المنهجية التي اتبعت للتحكم النشط في دوارات الرياح مبنية أساً سا على المحاكاة، وركزت على تبني نموذج مرونة هوائية لشفرة الدوار، هذا النموذج المقترح هو نموذج مرونة هوائية معدل، معروف في البداية باسم نموذج بيترز هي، ويتضمن نموذً جا حركيا إنشائياً، ونموذجاً للتدفق المستحث، مع نموذج للأحمال الهوائية. وتعتمد الحركية الهوائية وتأثيرات مقطع الشفرة على نموذج من نوع أونيرا وعلى تكامل حركيات الهيكل مع أحمال الهواء بما يسمح لهذا النموذج بتضمين التاريخ السابق لحركات الشفرة، استخدم الأسلوب أيضاً طرقًا تحليلية تقريبية مختلفة، مثل طريقة العناصر المحدودة، و طريقة رايلي-ريتز للحصول على مصفوفتي الجساءة والكتلة، وتم حل معادلة أويلر-بيرنولي للعوارض لإيجاد الاستجابة الحرة والقسرية بعد تحويلها إلى شكل مصفوفة فضاء الحالة، وذلك للحصول على أشكال الوضع والترددات الطبيعية، كما تم استخدام عارضة منتظمة كنقطة أولية للتحقق من صحة برنامج ماتلاب لطرق تحليلية مختلفة، وتمت مقارنة النتائج من

برنامج ماتلاب مع تلك الواردة في المواد المطبوعة، ووجد أن النتائج الخاصة بمصفوفتي الجساءة والكتلة متقاربة، وتم الحصول على نموذج فضاء الحالة لاستخدامه في تطوير آلية تحكم في الاهتزاز موثوق بها باستخدام التحكم بالمنظم التربيعي الخطي، وتم تعديل نموذج فضاء الحالة ليأخذ في الاعتبار الرقعة الكهروإجهادية الملتصقة بالعارضة لقمع الاهتزاز، وتظهر النتائج تحسناً في اهتزازات الحافة لنموذج دوارة الرياح، حيث يعزز هذا الأسلوب الفعالية الحقيقية للتحكم، ويدمج القوى والظروف الجوية بشكل فعال، وتوضح النتائج تحسنًا في التحكم في الاهتزاز الحاد لشفرة دوارات الرياح.

**كلمات البحث :**اهتزازات الحافة ، نموذج للمرونة الهوائية ، دوارات الرياح ، التحكم بالمنظم التربيعي الخطي

# CHAPTER 1

# INTRODUCTION

## 1.1 Potential of Wind Turbines

Wind power has immense potential as a possible renewable energy source. The power in the wind can be utilized as a non-polluting and renewable source of energy to meet energy needs around the world. Renewable and comparatively inexpensive energy sources have been the focus of modern world. The world is becoming more inquisitive about the wind potential and its future as a possible replacement to coal and oil in the energy sector [8]. According to an estimate by Arab Union of Electricity, the total installed capacity of Saudi Arabia in 2016 was 74.709 GW which is expected to rise to about 100 GW in 2027 and about 74% is currently generated from thermal resources including gas, oil and diesel [9]. According to vision 2030, an initial target for renewable energy generation was set at about 9.5 GW and by 2040 the goal is to generate more than 50% (about 72 GW) from renewable energy resources [10, 11]. The wind energy has

immense potential in Saudi Arabia as it is blessed with extensive wind corridors, lengthy shores and relatively high wind speeds. According to an estimate by King Abdullah City for Atomic and Renewable Energy, the mean wind speed in most of Saudi Arabia is between 6.0 to 8.0 m/s [12]. In another study, the wind speed was measured at a height of 40 m at five different locations namely Arar, Dhahran, Dhulum, Gassim and Yanbu in Saudi Arabia and it was found that the average wind speed varies between 4.3 to 5.7 m/s. [13]

After careful assessment of future energy needs, it was found that there is a need to initiate major developments in both design and operation of wind turbines. Moreover, the cost of energy production, using wind as a main resource, has been dropping considerably since the last two decades. The cost reductions are mainly due to introduction of newer technologies and higher production scales which are consequently leading to larger, more efficient and more reliable wind turbines. According to an estimate, the cost of energy from wind turbines tend to vary from $3 - 6 per Watt for relatively small wind turbines to 15 - 20 Cents/kWh for large turbines [14]. A recently published paper promised even more economical per unit cost varying from 5.85 Cents/kWh in Dhahran to 12.81 Cents/kWh in Riyadh while using the most feasible wind turbines for the region. [15]

## 1.2   Types of Wind Turbines

A wind turbine basically converts the kinetic energy of wind into mechanical power of wind turbine, through rotation about some axis, which is subsequently

transformed into electricity by a generator connected with the main grid. Rotating design can be further classified into two great classes of wind turbines, horizontal and vertical axis wind turbines. Horizontal-axis wind turbines (HAWT) spin about a horizontal axis while a vertical-axis wind turbine (VAWT) spins about a vertical axis [16].

**Horizontal Axis Wind Turbine**

Horizontal Axis Wind Turbine (HAWT) uses lift as the main driving force and have been found much more efficient than VAWT. The rotor of HAWT is usually mounted on a hub and tower structure and responds to the changes in wind direction and turbulence which have a negative effect on performance. The best locations for HAWTs are open areas with smooth air flow and few obstacles. [6, 17]

**Components of HAWT**

The main components [17] of the wind turbines are as follows

- Rotor Blades
- Hub
- Gearbox
- Shafts

- Nacelle
- Tower
- Brakes
- Controller

- Yaw Mechanism
- Alternator
- Anemometer

## 1.3  Rotor Dynamics

**Rotor**:

A rotor is a body suspended by a set of cylindrical hinges or bearings that allow it to rotate freely about an axis fixed in space.

**Examples of Rotor**:

Wind turbine bladed disks, Transmission Shafts, parts of reciprocating machines, Space vehicles & celestial bodes, gas turbines, Steam turbines, pumps, compressors, turbochargers, electric motors and generators, etc

**Wind Turbine Rotors**

The rotors can be divided into two major types depending upon the type of motion. A wind turbine rotor undergoes periodic vibrational motion under aerodynamic loading. Moreover, It is a fixed rotor as it has fixed bearings with a limit on angular velocity. The other type are isolated rotors which are mainly governed by the laws of conservation of linear and angular momentum. If small displacement and rotations could be assumed, both fixed and free rotors can be treated similarly [18].

Wind turbine rotors are the main rotating part of wind turbines and are usually shaped like an aerodynamic body with an airfoil as its cross-section. The airflow over the blades generates momentum and lift which consequently causes them to rotate and vibrate. The blades on most modern wind turbines are made from composites materials such as fiberglass reinforced plastics and wood/epoxy laminates.

The rotor blades are usually subjected to most stringent structural requirements as they are the most basic load bearing component in HAWT. In addition to the primary requirements of stiffness, strength, and ease of manufacturing, turbine blades must withstand severe fatigue loading under disparate environments. Fatigue is the main factor that reduces the life span of wind turbine and can be defined as the progressive and localized structural damage that occurs when a material is subjected to cyclic loading or stresses. Therefore, possible causes of failure (breakdown) of wind turbines have to be considered while designing wind turbine blades. The turbine blades are made up of certain types of composite materials in which low strain damage failure can occur when subjected to cyclic loadings under gust conditions. To avoid this and other kind of failures, design engineers have to incorporate some safety limits by employing various controller mechanisms [6].

### 1.3.1 Rotor Coordinate System

The motion of a rotor system can be represented using fixed (inertial) Cartesian coordinate system (x,y,z) on a beam as shown in Figure 1.1. The x-axis represents the shaft's axis and the y- and z-axes form a plane perpendicular to the shaft. The origin, o, coincides with an arbitrarily defined reference position of the shaft centerline. The lateral motion of the shaft is then defined by translations and rotations (using the right-hand rule) in the (x, y)-plane. Small motion assumptions are generally made so both the translational $(u, v, w)$ and rotational components

$(\alpha, \beta, \theta, \gamma)$ of motion may be treated as vector quantities.
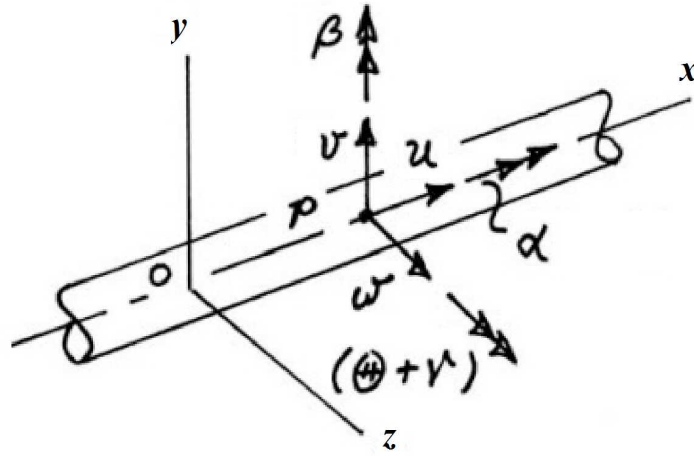


Figure 1.1: Rotor Coordinate System representing translations and rotations[4]

The displacement of a typical structural point on a rotating assembly includes axial, lateral, and torsional components. The associated translation and rotations are as follows:

- Axial Components: translation $(w)$

- Lateral Components: translation $(u, v)$ and rotation $(\alpha, \beta)$

- Torsional Components: superposition of rigid body rotational and torsional deformation $(\theta + \gamma)$

The torsional motion is usually represented as a superposition of a rigid body rotation $(\theta)$ plus a torsional deformation $(\gamma)$. In most rotor systems, the axial components of motion, $w$, is actually negligible. In addition, the static and dynamic coupling between the torsional motion $(\gamma)$ and lateral components of motion

($u$, $v$, $\alpha$,$\beta$) are generally weak. Thus, most rotor system model treat the lateral vibration and torsional vibration problems as separate and decoupled problems.

For the case of geared systems, however, there may be strong static and dynamic coupling between the torsional and lateral motions of the rotating assemblies [4].

## 1.4   Vibrations in Wind Turbines

Rotors with blades, as in HAWT, are prone to edgewise vibrations due to the flexibility of the blades and the support. The current challenge is to significantly reduce the cost of wind energy by increasing the expected lifetime of wind turbines through implying mechanisms which reduce fatigue loads. The detrimental effects of edgewise vibrations, with increase in the size of wind turbines blades, has been the focus of various researchers as they significantly decrease the fatigue life of wind turbine blades [19]. Most turbine blades have a design life of about 30 years, however, this can be reduced to 10 years of service due to presence of high fatigue loads [20]. The conventional way of reducing fatigue loads is by pitch regulation of turbine blades as shown by Bossanyi in [21].

### 1.4.1   Modes of Vibrations

In order to model a wind turbine blade for vibration study, the nature of the dynamic equation for the edge-wise and flap-wise vibration needs to be understood. Wind turbines have two major modes of vibrations, namely edge-wise and

flap-wise vibrations [5] as shown in Figure 1.2. The edge-wise vibrations, also known as lead-lag, are oscillations in the plane of rotating axis of wind turbine. The overall coordinate system and the direction of rotation is shown in Figure 1.7. Most researches use both active and passive vibrational control to increase expected lifetime of turbine blades.
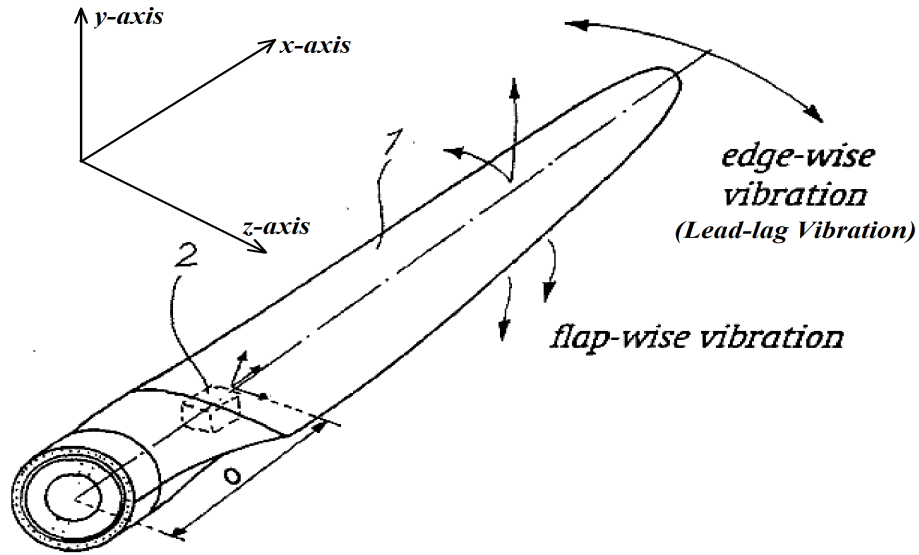


Figure 1.2: Edge-wise (Or lead-lag) and Flap-wise Vibrations in wind turbine blade [5]

## 1.4.2 Whirling Motion

Whirling of a shaft is its motion in a direction transverse to the axis of rotation. For a point mass in the rotor system, Whirling can be defined as a simple harmonic motion which occur simultaneously in two perpendicular directions with common frequency ($\omega$) known as whirl frequency. This frequency is also equal to the average precessional rate over a complete rotation. A synchronous whirl (circular vibrational motion) is one in which the shaft rotates and spins about its axis and

both rotational speeds are identical. There are two types of whirling motion based on frequency:

- Free-vibration motion at a natural whirl frequency (Free whirling)

- Forced Vibrations at a specific excitation frequency

In elliptical vibrational motion, acceleration is always directed towards the center of the elliptical orbit while the transverse acceleration component is negligible. This motion reduces to circular motion in case of isotropic support properties [18]. The two special cases of elliptical vibration motion are forward circular whirl and backward circular whirl. Forward circular whirl is the normal motion of a rotor and it is the motion occurring in the same direction of the spin speed while backward circular whirl occurs infrequently except for systems that have coupled counter-rotating assemblies [4]. A forward motion is characterized by positive whirl angular velocity $\omega_w$ while a backward motion is characterized by a negative value of $\omega$. The natural frequency of the rotor or the whirl speed does not depend on the rotational speed $\Omega$ [18].

## 1.5    Aerodynamics of Wind Turbine

There are numerous aerodynamic models for wind turbines and while most of them are effective in providing an estimate of the overall performance, only few are capable of determining aeroelastic behaviour. This is because the determination of aeroelastic behaviour requires greater amount of accuracy along with consideration

of dynamic effects such as dynamic stall and induced inflow. In this section, some of the aerodynamic models are briefly reviewed along with some basic concepts relating to these models.

### 1.5.1  Blade Element Momentum Theory

This theory is quite popular and require relatively less computation as it presents set of linear equations that can be solved iteratively to get the performance parameters. It is a combination of momentum and blade element theory as summarized in figure 1.3. It calculates the performance characteristics of an annular section of an idealized rotor as shown in Figure 1.4. The result is than obtained by integrating the values obtained for each annular section of the rotor.
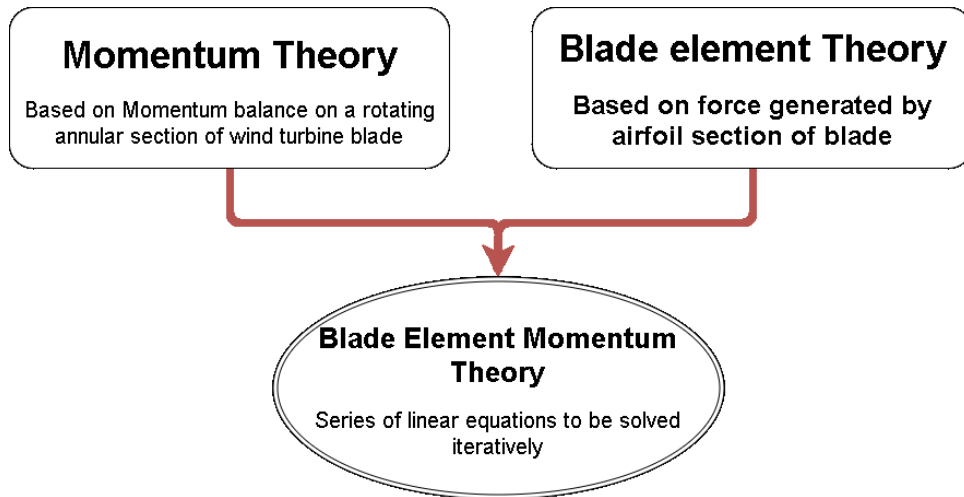


Figure 1.3: Simplified Block Diagram for Blade Element Theory
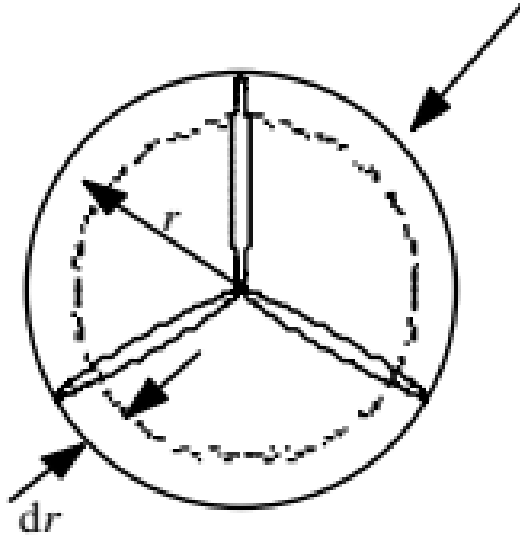
Figure 1.4: Annular Section formed by differential radius ($dr$) of the rotor [6]

## 1.6    Aeroelasticity

Aeroelasticity can be described as a study about the effect of aerodynamic loadings on various elastic bodies such as wind turbine blades which deform significantly under cyclic loading. The aeroelastic model should be able to predict forces on a rotating isolated blade considering the fluid-structure interaction. In aeroelastic problems such as that of a wind turbine blade, the response of the system under external loadings is needed to be determined [22]. These loadings are of various types including centrifugal, angular acceleration, aerodynamic and other external forces. The centrifugal forces are caused by body inertia and is directed away from the center of the rotor. The angular acceleration forces are mainly caused by rate of change of angular velocity of wind turbine rotor. The aerodynamic forces are primarily caused by airflow relative to the blade which include steady wind conditions, gusts and turbulence such as Kelvin-Helmholtz instabilities [23]. In

this research, the primary response to be controlled are the edgewise displacements which are mainly caused due to combination of all these forces. These vibrations, as described earlier in section 1.4, are caused due to varying wind conditions and hence wind turbine blades can be better modelled as a dynamic response problem accommodating aerodynamic, inertial, angular acceleration and other external forces.

### 1.6.1 Static Aeroelasticity

The wind turbine blades has a typical airfoil section and its aeroelastic behaviour largely depends on aerodynamic forces acting on blades. The aeroelasticity induce changes in angle of attack ($\alpha$) which subsequently results in change in forces. In order to incorporate the aeroelastic effect, a typical blade cross-section can be represented by a flat plat airfoil attached to a torsional spring as shown in Figure 1.5. Also, the forces on a typical wind turbine airfoil are shown in Figure 1.6

## 1.7 Control System

Control system analysis and design in general can take place in either time or frequency domain. The physical variables that are directly observable and measurable can be analyzed in time domain while in frequency domain these quantities undergo some transformation before computation.
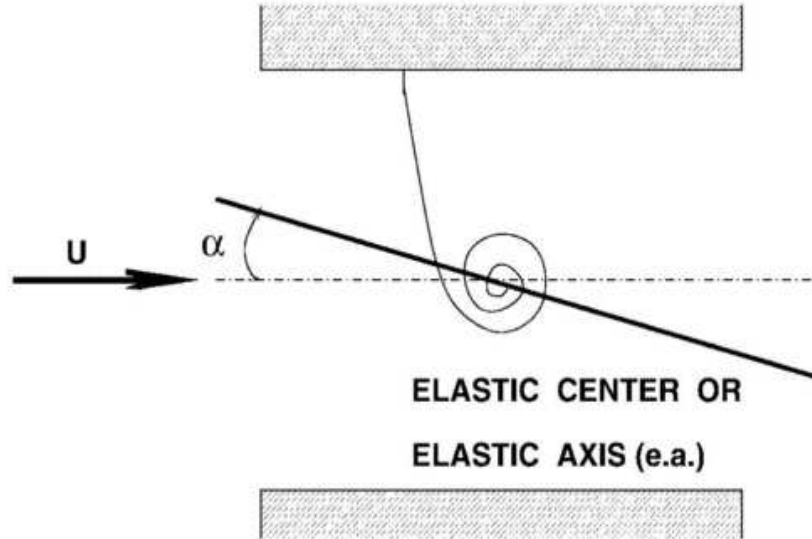
Figure 1.5: Simplified aeroelastic model of an airfoil [7]

## 1.8    Smart Materials

Individual pitch control of blades is one method to minimize fatigue loads. Other methods include the use of aerodynamic control surfaces such as trailing edge flap and Microtabs which are not effective in controlling the displacements within the plane of rotation. Researches presents various ways of active control methods for HAWT and suggests that intelligent control systems using smart materials can significantly reduce the in-plane vibrations [24].

Piezoelectric materials are specialized crystals with the ability to generate an electrical charge when stimulated by an external stimuli like temperature, force, electric and magnetic field or vice versa, hence, they can be used both as sensors and actuators [25]. These Piezoelectric based actuator/sensor combination is usually coupled along the span of the blade. The actuator apply localized strains/displacements based on signal from sensor and control law [26, 24].

13
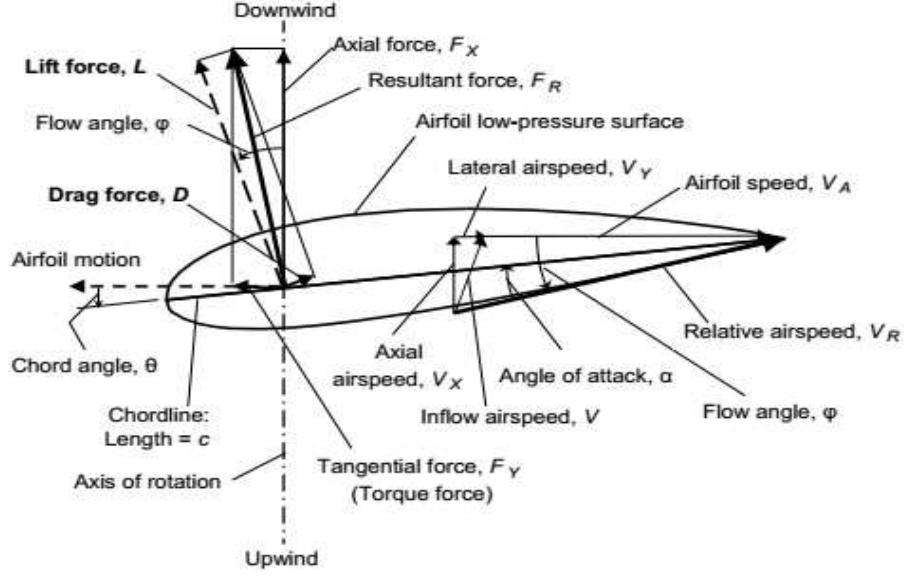
Figure 1.6: Forces on airfoil

In order to model such system, we can either use electrical energy balance equation or constitutive relations. Smart materials have coupling between the electric and elastic fields which can be represented by linear constitutive equations given below.

$$\vec{D}_e = \varepsilon_0 \vec{E}_f + \sigma_p \vec{\varepsilon_e} \tag{1.1}$$

$$\vec{\sigma_e} = -\sigma_p{}^T \varepsilon_0 + C_e vec\varepsilon_e \tag{1.2}$$

Where $\vec{D}_e$ is the electric displacement vector, $\vec{E}_f$ is the electric field vector derived from the negative gradient of the electric potential, $\varepsilon_0$ is the dielectric permittivity matrix evaluated at constant elastic strain, $\sigma_p$ is the piezoelectric stress matrix, $\varepsilon_e$ is the elastic strain vector, $\sigma_e$ is the elastic stress vector and $C_e$ is the elastic matrix (Hook's law) at constant electric field. The moment (both elastic and

14

piezoelectric) acting on the structure can be obtained in terms of input voltage by integrating the first equation over the depth of typical actuator patch. The deformation of the structure in terms of output voltage and the strain can be obtained by integrating the second equation over the depth of a sensor patch [27]. Researchers have suggested some active vibration control models [28] that attempts to improve on the modelling with a better controller that works in a more efficient way to enhance the lifetime of the wind turbine.
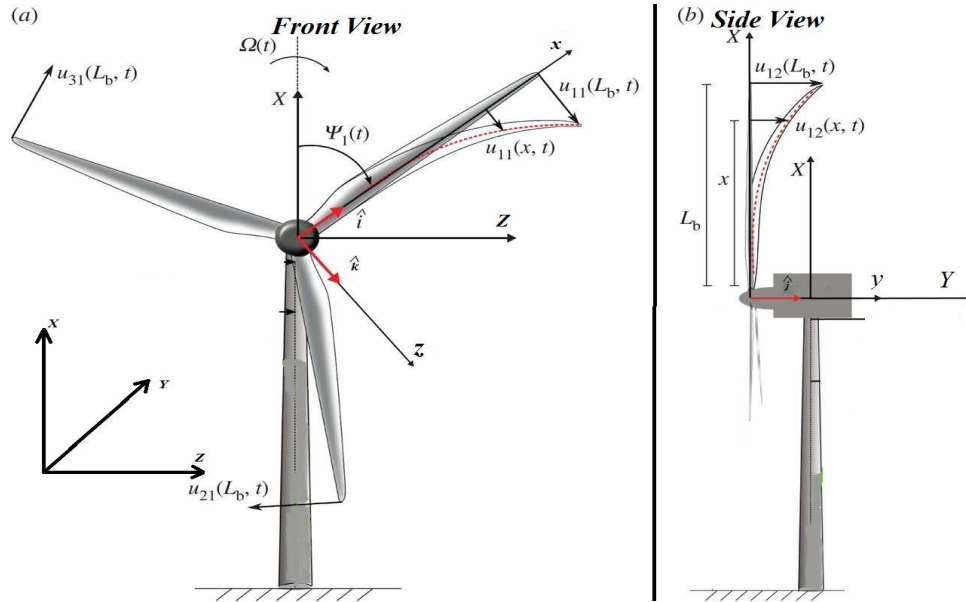


Figure 1.7: Overall Direction of Rotation, Coordinate axis, velocity direction for HAWT (Not Drawn to Scale)

## 1.9  Problem Statement

The problem which is currently being faced is that in order to develop a responsive control based on smart materials, i.e. one that significantly reduces edge-wise vibrations, a better and more realistic aerodynamic model should be

used. This would greatly improve the accuracy of forced response simulations and would eventually help to formulate a control feedback technique that effectively reduces vibrations. This could prove significant in increasing wind turbines life and lowering the overall cost. Hence, the problems are two-folds, mainly, a realistic aerodynamic modelling of wind turbine and formulating a viable control based on that mathematical model.

# CHAPTER 2

# LITERATURE REVIEW

The subject of aeroelastic beam modelling for vibration control is a diverse subject and hence requires knowledge from various fields including aerodynamics, engineering vibrations, elasticity and control. Hence, considering the diversity of the topic and organization, the section of literature review is divided mainly into four major sections.

1. Beam Vibrational Model

2. Aeroelastic Model

3. Simulation based Modelling

4. Control Techniques

## 2.1   Beam Vibrational Model

Khulief and Bazoune [29] developed a Finite Element (FE) model for vibration analysis of a rotating tapered Timoshenko cantilever beam with variation in taper

ratio and beam length. The method used reduced set of modal co-ordinates and was formulated for isotropic, homogeneous material with a beam of rectangular cross-section. Mathematical expressions for mass and stiffness matrices were obtained while taking into account the centrifugal stiffness effects due to rotation of beam. Vibrational modes for different boundary conditions were validated by comparison with published numerical results. In [30], a reduced set of modal co-ordinates were obtained for a rotating elastic beam using transformation from nodal to the modal co-ordinates space. The concept of potential and kinetic energy from Lagrangian energy method was employed to obtain finite element mass and stiffness matrices. This choice of realistic set of modal co-ordinates enhanced the efficiency of the FEM and a comparison was made for the efficiency of the optimal control with and without rotational effects.

Baillargeon [31] performed experimental and 2-D finite element vibration analysis for a Aluminum sandwich cantilever beam using ABAQUS/Standard 6.3-1 and implemented active feedback PID control through piezoelectric shear actuators. The results were validated through comparison of natural frequencies (1st four) of the experimental and finite element model and significant decrease in hybrid cantilever beam vibrations was observed after implementation of PID controller. Gunda et al. [32] implemented super-element FE technique to reduce the degree of freedom for dynamic analysis of rotating tapered uniform cantilever beams using Fourier-p approach. In order to obtain natural frequencies, a combination of polynomials and Fourier series were used as shape functions. This technique

18

significantly decreases computational time and comparable non-dimensional natural frequencies results were obtained using a single super-element under different rotational speeds. Research further suggested that the technique can be implemented in FE modelling of rotating beam with airfoil cross-section. Wereley et al. [1] develops and validates a uniform and non-uniform rectangular isotropic cantilever beam model. A MATLAB code was formulated for isotropic uniform beam and mode shapes were obtained using assumed modes, lumped parameter and finite element method. The effect of piezoelectric patches were included for the non-uniform case and the results showed that assumed mode method closely matches with experimental results for both beam types.

| # | Source | Mathematical Model | Material Type | Methodology |
|---|--------|-------------------|---------------|-------------|
| 1 | Bazoune & Khulief, 1992 [29] | Derived 4 DOF FEM for vibration analysis of a rotating rectangular tapered Timoshenko cantilever beam. | Isotropic, homogeneous material | Mass and Stiffness matrix were developed including centrifugal stiffness effects. Free vibrational modes for both fixed and hinged end conditions were obtained. |
| 2 | Khulief Y A., 2001 [30] | FEM model was developed and reduced set of modal co-ordinates were obtained using transformation to the modal co-ordinates space. | Uniform, Isotropic and homogeneous | Model was developed using Lagrangian energy method. Mass and Stiffness matrix includes centrifugal stiffness effects |
| 3 | Baillargeon, 2003 [31] | 2-D finite element vibration analysis | Aluminium (Isotropic, homogeneous material) | Experimental analysis and simulation using ABAQUS/Standard 6.3-1 software |
| 4 | Gunda et al., 2007 [32] | Reduced DOF using super-element FE technique for rotating tapered cantilever beam using Fourier p approach | Uniform Isotropic, homogeneous material | Polynomials and Fourier Series shape functions were used |
| 5 | Wereley, 2011 [1] | Used Euler-Bernoulli beam equations to develop a model for non-rotating cantilever beam | Uniform (Isotropic, homogeneous material) and non-uniform with PZTs effect | Assumed Modes, Lumped parameter and FEM methods were used to obtain mode shapes and natural frequency |

Table 2.1: Summary of the Beam Vibrational Models for Wind Turbines blades.

## 2.2 Aeroelastic Model

Prediction of forced response requires an accurate estimate of aerodynamic forces over the wind turbine blade. The flow around a turbine blade involve both changes in position and rotation. Under dynamic conditions, flow tends to approach a stable flow pattern after an initial transient period. Fung in [22] obtained an analytical solution for a fully attached flow for the oscillating airfoil motion accounting also for change in position. Leishman in [33] presented both analytical solution and experimental results which indicates lift lag or double stall phenomenon during fully attached conditions with a higher lift at decreasing $\alpha$ and relatively lower lift at increasing $\alpha$ as compared to the flow over a non-rotating airfoil . Hence, the wind turbine blade dynamics requires the periodic modeling of aerodynamic forces. Numerous dynamic stall models have been suggested as discussed and suggested by researchers to account for these dynamic effects. Current research divides the dynamic stall models into three categories based on the approach that is being used to model the forcing function. These approaches include the effects of different flow conditions over the wind turbine, the characteristics of the lift curve and dynamic angle of attack [34].

Beddoes and Leishman [35] formulated a dynamic stall model for a rotating helicopter blade and accounted for separated and attached flow effects over a rotating blade cross-section. The model was mainly formulated for helicopter rotor dynamics and include variations in flow response as parameters like Mach number change. Hansen et al. [36] developed a reduced DOF Beddoes-Leishman model

ignoring the effects of compressible flow and leading edge separation while aiming to account for the effect of the flow conditions around turbine blades. [31] Nour et al. [37] used FEM to obtain natural frequencies and mode shapes of helicopter blades made of various materials subjected to static aerodynamic load. Analytical and numerical modeling depicts the difference between stresses and various spectrum of displacements of orthotropic and isotropic materials. Liu [38] defined the appropriate coordinate system and developed coordinate transformation relations to derive the equations of motion for elastic rotating beam with constant angular velocity. A distributed aerodynamic forces and moments model was developed to yield a state-space model for aerodynamic loads. The analytical expressions for strain energy, external work were also obtained with rotational velocity effect included in kinetic energy. The technique was found to reduce effectively both noise and vibrations in helicopter blades with active and passive adaptive control. Larsen et al. [34] developed and validated a wind turbine aerodynamic model for lift under dynamic stall and made a comparison between different aerodynamic lift models including Beddoes-Leishman and the ONERA model for various wind turbine profiles subjected to different dynamic effects under certain loading conditions. Svendsen et al. [39] used dynamic stall aerodynamic model from [34] and developed an active control for vibration modes of a HAWT. The control system consists of actuator-sensor pairs on each of the blades, and targets a set of three modes. The control signals from the blades tuned the response of the actuators to provide resonant damping of three modes. Numerical simulations were validated

by experimental data and show that active damping system can provide a significant reduction in the response amplitude of the targeted modes. Similarly, in [40] Nailu and Balas devleoped a rotating blade mathematical model with dynamic aerodynamic coefficients calculated using Beddoes-Leishman dynamic stall model. Adaptive Controller was designed and validated for the model to control flutter vibrations using flap under periodic aerodynamic loads.

Roura et al. [41] focused on development of an aero-elastic model using vortex panel method to predict the effect of near and far wake by coupling BiotSavart law with rotor aerodynamics. Numerical code was formulated using relaxation method with periodic boundary condition and validated against published experimental results. In 2011, Jeong et al. [42] developed nonlinear beam FE model to perform aero-elastic analysis of Wind Turbine blades through vortex method to estimate forces, deformations and their effect on aero-elastic stability. This study used nonlinear beam theory model for the structural analysis to account for significant structural non-linearities that exist in large wind turbines. Aeroelastic analyses of wind turbine blades were conducted using the vortex method. In vortex model of the rotor blades, trailing and shed vorticity in the wake are represented by lifting lines. The strength and position of the vortices from the induced velocity were found using the Biot-Savart law. Hence, an aero-elastic model was developed and both stiffness and aerodynamic matrices were obtained. A verification and validation of vibration mode was performed by comparing the aero-elastic model to previously published computational results and they were found to be in excellent

agreement with the previously publish results as well as experimental data. In 2013, Zou et al. [43] formulates a numerical vortex type aerodynamic model for an airfoil subjected to time varying loads and aero-elastic instabilities. Lift and drag predictions at high angles of attack of the Vortex aerodynamic model are validated with experimental and CFD results. Subsequent aero-elastic simulations concluded that beyond certain wind velocity the edge-wise vibrations surge both due to negative damping and lock-in phenomenon. Skrzypinski[44] developed an aerodynamic and CFD model for a wind turbine to predict vortex and stall-induced vibrations of wind turbines in parked condition. The results suggest that further aero-elastic analysis and simulations are required to predict blade vibrations in parked conditions. Hence, suggesting an area that can be worked upon by future researchers.

In [45], Bichiou et al. coupled a 2D quasi-steady approximated aerodynamic model with an airfoil section to determine the effects of structural and dynamic non-linearities on using Hopf bifurcation near the onset of instability. Using the Numerical simulations of the approximated model, flutter speed was shown to be varied with parameters such as initial conditions, limit-cycle oscillations, rotational speed and blade radius. Wenzhi and Jianxin [46] employed Blade element momentum (BEM) theory to present a modified Wilson optimized model of a turbine blade for a wind turbine. Aerodynamic coefficients and their dependency on factors such as cost, craft, structure and blade aerodynamic parameters was found. 3D modelling of the turbine blade was carried out using CAD software.

The model can be further used for aerodynamic, FEM, dynamic simulation as well as a CNC machine model. In [47], Staino et al. use Euler-Lagrangian approach to develop an aerodynamic mathematical model for a blade with embedded active actuators to control edgewise vibrations through Linear-quadratic (LQ) control law. The blade mathematical model was a Bernoulli-Euler cantilever beam rotating at a constant rotational speed and accounts for the structural properties like stiffness per unit length, mass, gravity, centrifugal stiffness and the overall interaction between tower and the blade. The model takes into account the variations in aerodynamic loads under different wind conditions using modified Blade Element Momentum (BEM) theory. Numerical solutions were then carried out and compared with the experimental data and show promising improvement in the control performance and vibration suppression. Bernhammer and De Breuker [48] develop and validated a geometrically non-linear wind turbine structural FE model using blade element method (BEM) which reduces structural degrees of freedom. Ther aerodynamic loads were obtained from [49] using an aeroelastic tool for wind turbines known as DU SWAT. The 6 rigid body modes were obtained and used to describe deformation and compatibility between different components of wind turbines.

Alpay et al. [50] validates a nonlinear static and dynamic aerodynamic model of a HAWT blade using FEM with coupling between rotations and deformations. The research used a simple dynamic linearly varying aerodynamic force model acting along the span of the turbine blade. It uses floating frame approach and

studies the effect of various parameters on deformation such as coupling between inertial forces, bending and blade skin.

Peters et al. in [51], presented a detailed hierarchical aeroelastic model for a rotating helicopter blades using the ONERA dynamic stall model. The aeroelastic model considers the coupling between the structural-dynamic model, induced flow model and a derived airloads model using an extension of thin airfoil theory by Theodorsens approach. The shape functions are used to represent inflow model and are converted to closed-form state-variable equations which are ideal for aeroelastic modal analysis.

| # | Source | Aeroelastic Model | Loading Condition |
|---|--------|-------------------|-------------------|
| 1 | Leishman and Beddoes, 1989 [35] | Developed a semi-empirical *dynamic stall* model for helicopter blade section for unsteady lift, drag and pitching moment. | Pitching and Plunging Motion |
| 2 | Fung, 1993 [22] | Presented an overview of 2D oscillating airfoil theory and fundamental equations for fully attached flow using *Theodorsen function* | Vertical Translational and Rotational Oscillations |
| 3 | Peters and Barwey, et al., 1994 [51] | Used *ONERA* type model for flow around helicopter blades | Rotating Motion |
| 4 | Hansen and Gaunaa, et al., 2004 [36] | Developed a reduced linearized *Beddoess-Leishman* dynamic stall model for helicopter blade section by ignoring leading edge separation | Heaving, lead-lag and pitching Motion |
| 5 | Wenzhi and Jianxin, 2009 [46] | Used Wilson optimized BEM model for designing and subsequently calculating aerodynamic coefficients for turbine blade | Only Rotational Motion |
| 6 | Larsen, 2007 [34] | Presented a dynamic stall model for Wind turbines and compare results with *ONERA* and *Beddoess-Leishman* dynamic stall model | Both attached and stalled aerodynamic loading conditions under Rotational motion |
| 7 | Svendsen, 2011 [28] | Used *Larsen model* in [34] to develop a 3D aeroelastic vibration model of a single blade as well as for complete wind turbine. | Aerodynamic forces under Rotational motion while including centrifugal effect as in [34] |
| 8 | Nour and Gherbi, et al., 2012 [37] | Developed and simulated a *FE model* of helicopter blades made of different materials to calculate mode shapes and natural frequency | Aerodynamic loads included the effect of centrifugal force with varying rotational speed |
| 9 | Staino and Basu, 2012 [47] | Used modified BEM model and Euler-Lagrange beam model to develop aeroelastic model for 5 MW wind turbine blade | Accounts for Centrifugal stiffening, gravity and interaction between blade and tower |
| 10 | Li and Balas, 2013 [52] | *Beddoess-Leishman* dynamic stall model | Periodic aerodynamic Loading under rotational effect |

Table 2.2: Summary of the Numerical Aeroelastic modelling of Wind Turbines blades.

| # | Source | Aeroelastic Model | Loading Condition |
|---|--------|-------------------|-------------------|
| 1 | Liu, 2005 [38] | Developed a *Vortex* based simulation model for BVI induced vibrations and noise suppression of a helicopter blade using an actively controlled flap technique. | Accounted for blade flexibility and used distributed model of aerodynamic force and moment under Rotational Motion |
| 2 | Roura and Cuerva, et al., 2009 [41] | Used *Vortex panel method* to develop a numerical code for near and far wake of 3D rotor and coupled Biot-Savart law with Rotor dynamics to determine tip vortices | Periodic aerodynamic loadings under rotational effect |
| 3 | Alpy and Barut, 2010 [50] | Used FEM to develop a non-linear static and dynamic aerodynamic model for a linearly varying force | Rotation and deformation coupling |
| 4 | Jeong and Yoo, et al., 2011 [42] | Developed a *FE model* for aeroelastic analysis of a large isolated wind turbines blade using Vortex method and non-linear beam theory | - Rotational effects were included while elastic effects were ignored |
| 5 | Skrzypinski, 2012 [44] | Used both analytical and CFD technique to predict vibrations due to the effect of vortex and stall for 2D and 3D airfoil models at standstill conditions | Loads under parked conditions |
| 6 | Zou and Riziotis, et al., 2013 [43] | Developed a numerical non-linear aeroelastic tool using Vortex method for an airfoil at high AOA (60°-120°) | Dynamic loads along with aeroelastic instabilities at parked conditions for different speeds |
| 7 | Bichiou and Abdelkefi, 2014 [45] | Used Numerical simulation for 2-D quasi steady flow using normal form of Hopf bifurcation near instability region for an airfoil | Plunging and Pitching Motion |
| 8 | Bernhammer and De Breuker, 2014 [48] | Used modified BEM and beam theory to develop non-linear wind turbine model using *DUSTWAT* FE tool | - |

Table 2.3: Summary of the Simulation based Aeroelastic modelling of Wind Turbines blades.

## 2.3 Simulation based Modelling

In [53] Wang et al. presented a nonlinear beam FE mathematical composite beam model using geometrically exact beam theory (GEBT) and spatial discretization technique. The numerical simulations for displacements were carried out using BeamDyn software and are validated through simulating vibration solutions for static and dynamic composite cantilever beam with rectangular cross-section. Couturier et al. [54] developed a method to get 6 DOF stiffness matrix for a general cross-section anisotropic beam. The stiffness matrix is used in FEM analysis which is validated by comparing deformation modes. The model is found to be accurate and fewer elements were required to obtain satisfactory mode shapes for wind turbines blades.

Kumar et al. [55] formulated a Al 2024 based wind turbine blade design and simulated the CAD model on ANSYS software for vibrational response at above and below survival speed. The maximum deformation occurred at tip when the turbine blade was subjected to forced vibration with free-free and fixed-free boundary conditions. Buren et al. [56] performs modal analysis using ANSYS FE software and validates results with a derived analytical model for a hollow cylinder. Wind turbine isotropic blade modal analysis is than performed in order to find mode shapes. In part II, Buren et al. [57] develops and verifies an error bounded isotropic FE model of CX-100 HAWT and obtain vibration solution using Gaussian process models. Using test analysis correlation (TAC), error quantifica-

tion and statistical methods such as Phenomena Identification and Ranking Table (PIRT), the model code has been found to predict with great accuracy the bending and mode shapes for different types of boundary conditions when compared with experimental results. Leung developed governing equations for pre-twisted helical anisotropic beam with rectangular cross-section with fixedfixed, fixedfree and freefree boundary conditions. The results were compared after the vibration solution was obtained through Galerkin method with a pre-twisted straight beam model in ANSYS [58]. Garinis et al. [59] obtained the natural frequencies and mode shapes for composite helicopter blades using Lanczos method on ANSYS software. In [60] Buren et al. quantifies the amount of uncertainty in a non-linear FE beam code (NLBeam) based on geometrically exact beam theory. The mode shapes for different beam configuration and boundary conditions were compared to establish the credibility of NLBeam. The study compares a three dimensional shell model and a simplified one dimensional beam model. Experimental modal analysis were also performed and the results were than compared with those obtained from NLBeam software for both free-free and fixed-free boundary conditions. The results demonstrate that the simplified beam models are capable of replicating vastly different experimental configurations. The research also suggest that, in order to study the nonlinear behavior more accurately, the assumption of a wind turbine blade as a simplified cantilever beam needs to be modified.

| # | Source | Model Type | Numerical Technique |
|---|--------|------------|---------------------|
| 1 | Wang and Sprague, et al., 2014 [53] | Used GBET through spatial discretization technique to model both static and dynamic rectangular composite cantilever beam. | Employed *BeamDyn* Software to implement Legendre spectral finite elements (LSFE) code for FEM analysis |
| 2 | Couturier and Krenk, et al., 2015 [54] | Developed **6 DOF** stiffness matrix for composite beam | - |
| 3 | Kumar and Dwivedi, et al., 2014 [55] | Developed a **CAD model** for a Wind turbine blade | Used *ANSYS* software and obtained results for free-free and fixed-free boundary conditions |
| 4 | Buren and Mollineaux, et al., 2011 [56, 56] | Isotropic Wind Turbine Blade and error bounded FE model | Mode shapes Gaussian process models Test analysis correlation error qualification using *ANSYS* |
| 5 | Leung, 2010 [58] | Galarkin method pre-twisted straight beam | pre-twisted helical anisotropic beam with different boundary conditions |
| 6 | Garinis and Dinulović, et al., 2012 [59] | Composite helicopter blades | Used Lanczos method |
| 7 | Buren and Mollineaux, et al., 2012 [60] | non-linear FE beam code NL-Beam | 3D shell model 1D model different beam config and B.C |

Table 2.4: Summary of the Simulation based modelling for Wind Turbines blades.

## 2.4 Control Techniques

Khulief and Bazoune in [61] also used active control method by implying two sets of sensors and actuators for suppressing vibrations of an elastic beam. Finite element results for vibrational modes were obtained through numerical simulations. Fei [62] succesfully employed and verified the effectiveness of the optimal PID and couple of feedback controller in active alleviation of vibration using PZT actuators for a homogeneous cantilever beam. Rotea et al. [63] designed active structure control of offshore floating wind turbines based on a reduced-order turbine model. The results are verified by carrying out the simulations of the system and the possible advantages and disadvantages of active control technique are discussed at the end. Nailu and Balas [52] formulate a robust and effective adaptive control technique for wind turbine with microtabs as modeled by Beddoes-Leishman and establish control law stability under different wind conditions.

Ali and Padhi [64] presented an optimal dynamic inversion approach for simply supported Euler-Bernoulli beam using non-linear PDE of motion. The governing equation were obtained using Hamilton principle and an exact expression for the control variable was developed. Numerical simulation showed the implementation of control law, which applied the force based on error between actual and desired state, effectively reduces beam transverse vibrations. Zhang [65] used a data-driven technique based on collecting drive train and tower acceleration measurements to develop a control law and analyze its mitigation effect on wind turbine vibrations by collecting a large set of experimental and on-field data.

| # | Source | Model Type | Control Technique |
|---|--------|-----------|-------------------|
| 1 | Khulief, 2001 [61] | **2 DOF** reduced order model for an elastic double-span $(2m)$ **rectangular cross-section beam** using FEM. | **Deterministic Optimal Control** technique using two sets of active control schemes |
| 2 | Fei, J. et al., 2010 [62] | Used FEM model for homogeneous steel **cantilever beam** $(0.8m)$ . | Developed **Optimal PID**, **Strain Rate Feedback** and **Positive Position Feedback Control** using bonded PZT actuators |
| 3 | Ali and Padhi, 2009 [64] | Used finite difference method to develop a numerical model for **non-linear Euler-Bernoulli PDE** for beam $(5m)$. | Implemented both continuous and discreet controller by employing **non-linear Optimal dynamic inversion control** |
| 4 | Li and Balas, 2013 [52] | Used **2 DOF** periodic time-varying **Beddoes-leishman aeroelastic model** for NACA 0012 airfoil $(0.27m)$ under various wind conditions . | Employed active microtab to implement **adaptive control technique** |
| 5 | Zhang, 2009 [65] | Employed various **data mining algorithms** to extract vibration data from real-time acceleration measurement from $1.5MW$ Wind Turbines. | Implemented **non-linear and non-parametric control** |
| 6 | Rotea, M A., et al., 2010 [63] | Used **reduced order wind turbine model** using FAST code for offshore wind turbines with a Rotor radius of $126m$. | Implemented **Loop Shaping Controller** (Robust Control) using Active Mass dampers (AMD) |

Table 2.5: Summary of the Control Techniques for Wind Turbines blades.

## 2.5 Current Status

1. After the literature review, it was observed that the modelling of an appropriate aerodynamic forcing function is an inspiring area for researches and offers great prospect for future research.

2. The challenge is to select and validate an appropriate aerodynamic model which would closely predict the actual wind turbine dynamic response.

3. The present BEM models are more efficient but there is a need to improve the accuracy by accounting for unsteady and harmonic motion of the blades especially due to rotor yaw, rotation speed, cross-section and twist along the span.

4. Future aerodynamic models may propose a hybrid approach, switching to vortex method when subjected to rotor yaw, which could prove more accurate.

5. Also, a suitable BEM would also account for the reduction in free stream velocity as the wind approaches turbine blades.

Hence, an aerodynamic model which would make this correction is required in order to improve the accuracy of dynamic response of models using BEM and get comparable results in dynamic conditions.

## 2.6 Objective

1. Develop a more realistic aeroelastic model that responds to real-time atmospheric conditions.

2. Development of a responsive control that significantly reduce edge-wise vibrations.

3. Improve the accuracy of the forced response simulations that are based on predicted aerodynamic forces.

### 2.6.1 Major Tasks

The major tasks of this work are hereby outlined below:

- Analyze the aeroelastic turbine blade models that were presented in the literature review and select a model which is not only efficient but would also help to improve the accuracy of wind turbine dynamic response.

- Propose an improvement on an existing turbine blade mathematical model by using Blade Element Momentum and Vortex Method.

- Estimate the aerodynamic force based on geometry, wind condition and other parameters which affects the wind turbine performance.

- Derive Beam equation in state space form for modified model.

- Formulate a code to find stiffness, mass and damping matrix from mathematical model.

- Solve for characteristics and dynamic behavior of turbine blades including mode shapes and natural frequencies.

- Implement LQR control technique to suppress wind turbine edge-wise (lead-lag) vibrations.

- Validate results using existing published numerical simulations and experimental data.

## 2.7 Procedure and Methodology

This research work would be designed to follow a sequence to make an effective mathematical model and eventually a controller. The first step naturally is to obtain kinematic representation of an aero-elastic, rotating composite beam using Euler-Bernoulli partial differential beam expression as given in Equation 2.1 and determine the appropriate initial and boundary conditions.

$$\frac{\partial^2}{\partial x^2}\left(EI\frac{\partial^2 w}{\partial x^2}\right) + \rho A\frac{\partial^2 w}{\partial t^2} + \frac{\partial}{\partial x}\left(T(x)\left(\frac{\partial w}{\partial x}\right)\right) = f(x,t) \qquad (2.1)$$

Where:

$T_c(x)$ - centrifugal tensile load at a distance x from the axis of rotation

The next step is to use the approximate analytical method such as Rayleigh-Ritz, assumed modes, lumped parameter and finite element method etc. to obtain the stiffness and mass matrix which can than be used to find natural frequencies and mode shapes of the system. The details of the applied method are presented

36

under the section of Rayleigh-Ritz Method.

At this step, an aerodynamic model would be formulated as suggested in literature review and described in problem statement. There are several aerodynamic approaches that exist in aerodynamic modelling and a study in this regard would include the following tasks:

- Select an aerodynamic technique for formulating load over wind turbine blade based on literature review.

- Use the technique to formulate an aerodynamic force expression in terms of relative wind velocity, rotation speed and geometry of turbine blade among other parameters. This would include

  - Defining different reference frames such as local and rotating etc.

  - Modelling the flow around the airfoil and along the span of turbine blade.

  - Account for dynamic conditions such as rotor yaw and induction at blades .

  - Make a comparison of the forcing function obtained from BEM and vortex Method.

- Formulating the expression into a matrix that can be used in state-space equation.

Different aerodynamic models were studied and one of them that is currently being used is presented under the section of current work. After getting the

aerodynamic expression from above, aerodynamic forcing function can be included in the equation of motions of the system obtained earlier. The next stage would include getting a state space model for the equations of motions (EOMs) developed in the previous step. This would help to obtain frequencies and mode shapes of the system for the forced uncontrolled response.

## 2.8  Objective of Predicting Aerodynamic Loads

A realistic aerodynamic model will help to achieve the following objectives:

- Determine allowable aerodynamic loading of the system

- Distinguish weakly aerodynamically damped edge-wise vibration modes from strongly damped flap-wise vibration modes.

- Improve performance of wind turbine blades under various wind velocity conditions

- Design an efficient controller based on more realistic vibration model

All these objectives, if achieved, would would eventually contribute towards increasing the overall life of wind turbine and lowering renewable energy cost.

The results of natural frequencies and mode shapes can be compared with published numerical and experimental data to verify the validity of the aerodynamic model. Generally, the geometric and material parameters of the wind turbines are taken from the published experimental data and are used to obtain the forced

response so that the results can be compared afterwards. This step is critical before controller design as it validates the effectiveness of the aerodynamic and mathematical model.

## 2.9   Controller Design

Controller forms an important step in the development of the project. Like controller design, this would normally start by obtaining the dynamic equation of the proposed beam model with bonded piezoelectric actuator and sensor combination. Hence, a dynamic equation for the smart structure will be obtained which would include the control force expression. Afterwards, applying the state space method and piezoelectric theory, a state space model would be obtained. In the next step, a transfer function can be obtained from this model and system can be modelled in MATLAB Simulink tool. The system can than be subjected to numerous conditions such as ramp, step and periodic inputs and the vibration response of system to these and other inputs can be modelled under LQR control technique as described in the earlier section. LQR control technique which make optimum use of actuator force, under various input conditions, is selected to dampen the vibrations.

Controller design is also a pivotal part of the vibration suppression in wind turbine blades as actuators dampens the vibrations significantly by generating the correct stimuli in a dynamic environment. The effectiveness of the controller depends on type of control technique, algorithm, number and position of actu-

ator/sensor combination among other factors. The challenge faced in this area is to design a cost, reliable, effective, robust yet efficient LQR controller that significantly reduce the overall vibrations.

The literature survey suggests numerous control techniques that are currently being used with most popular being PID and LQR controller. However, other techniques like Adaptive , Optimal and Fuzzy logic techniques were also found to be effective in reducing the vibration. The decision of controller was made based on results and LQR was found effective in reducing the vibrations. Hence, LQR controlled is suggested after testing the controller for the forced response of the wind turbine blade.

# CHAPTER 3

# STRUCTURAL MODELLING

## 3.1 Modelling of Beam

In case of a turbine blade, free and forced response can be modelled using various numerical techniques and natural frequencies and mode shapes can be obtained and a suitable control law can be formulated to suppress targeted modes.

The wind turbine blade can be modelled as a uniform cantilever Beam because the length of the large turbine blades is very large as compared to the other two dimensions and usually the aspect ratio is greater than 7 [66]. The dimensions of the beam were taken from the literature [1]. The beam considered here is made up of an isotropic, homogeneous material with a constant value of young modulus and density. This is taken as a case of validation for the development of the beam code in order to apply the Rayleigh-Ritz method on more complex problems later. The geometric and material properties of the uniform beam are summarized in the form of a table 3.1.

| Characteristic | Value |
|---|---|
| Length | 0.6128 m |
| Width | 0.0254 m |
| Thickness | 0.0106 m |
| Young Modulus | $6.9 \times 10^{10}$ Pa |
| Density | 2705 kg/ $m^3$ |
| Mass | 0.4456 kg |
| Moment of Inertia | $2.5089 \times 10^{-9}$ |

Table 3.1: The table summarizes the geometric and material properties for a uniform cantilever beam [1]

### 3.1.1 Governing Equation for Beam

The governing equation for forced transverse vibration for a wind turbine blades is Euler-Bernoulli equation which is also known as Dynamic beam equation (Euler-Lagrange Equation) [67] :

$$\frac{\partial^2}{\partial x^2}\left(EI\frac{\partial^2 w}{\partial x^2}\right) + \rho A\frac{\partial^2 w}{\partial t^2} = f(x,t) \tag{3.1}$$

For a uniform beam the above equation reduces to:

$$EI\frac{\partial^4 w}{\partial x^4} + \rho A\frac{\partial^2 w}{\partial t^2} = f(x,t) \tag{3.2}$$

For Free vibration, uniform beam case, the product EI is constant and hence the equation 3.2 can be rewritten as:

$$c^2\frac{\partial^4 w}{\partial x^4} + \frac{\partial^2 w}{\partial t^2} = 0 \tag{3.3}$$

Where:

$$c = \sqrt{\frac{EI}{\rho A}}$$

Two initial conditions and four boundary conditions are needed to obtain a unique solution of $w(x,t)$.

### 3.1.2 Moment and Forces

This section defines the moments and internal forces for beam axis given by Figure 3.1. The internal forces can be written in terms of stress

## 3.2 State Space Form

The Analytical solutions of Euler-Bernoulli beam Equation do not exist except for the simplest of cases. Hence, numerical solution is required along with an appropriate mathematical model to predict mass, stiffness and forcing term. For numerical simulation, PDE as in equation 3.1 are converted to state space form, and than the appropriate matrices are obtained. Hence, the Euler-Bernoulli equation is converted to state space equation which is given in [28] as follows:

$$M\ddot{u} + D\dot{u} + Ku = f \tag{3.4}$$

Where:

- D - Equivalent Damping matrix

- M  Equivalent Mass matrix

- K - Equivalent Stiffness matrix

- f  Forcing vector

## 3.2.1   Equivalent Mass Matrix

The equivalent mass matrix is a symmetric matrix and can be expressed in terms of area and longitudinal interpolation matrix as defined in reference in integral form (equation 3.5).

$$M = \int_L N_x^T \left( \int_A N_A^T N_A \rho dA \right) N_x dx \tag{3.5}$$

The area interpolation matrix is a function of y and z coordinates as given by equation 3.6

$$N_A(y,z) = \begin{bmatrix} 1 & 0 & 0 & 0 & z & -y \\ 0 & 1 & 0 & -z & 0 & 0 \\ 0 & 0 & 1 & y & 0 & 0 \end{bmatrix} \tag{3.6}$$

The integral term with area interpolation matrix in equation 3.5 can be expressed in terms of weighted area, section moments and moment of inertia of the beam.

$$\int_A N_A^T N_A \rho dA = \begin{bmatrix} A^\rho & 0 & 0 & 0 & S_z^\rho & -S_y^\rho \\ 0 & A^\rho & 0 & -S_z^\rho & 0 & 0 \\ 0 & 0 & A^\rho & S_y^\rho & 0 & 0 \\ 0 & -S_z^\rho & S_y^\rho & I^\rho & 0 & 0 \\ S_z^\rho & 0 & 0 & 0 & I_{zz}^\rho & -I_{zy}^\rho \\ S_y^\rho & 0 & 0 & 0 & -I_{zy}^\rho & -I_{yy}^\rho \end{bmatrix} \tag{3.7}$$

Where:

$$
\begin{aligned}
A^\rho &= \int_A \rho dA \\
S_y^\rho &= \int_A y\rho dA \\
S_z^\rho &= \int_A z\rho dA \\
I_{yy}^\rho &= \int_A yy\rho dA \\
I_{zz}^\rho &= \int_A zz\rho dA \\
I_{zy}^\rho &= \int_A zy\rho dA
\end{aligned}
$$

The longitudinal interpolation matrix can be defined in terms of shape function

in s domain.

$$N_x(x) = \begin{bmatrix} N_1^a & 0 & 0 & 0 & 0 & 0 & N_1^b & 0 & 0 & 0 & 0 & 0 \\ 0 & N_q^a & 0 & 0 & 0 & N_r^a & 0 & N_q^b & 0 & 0 & 0 & -N_r^b \\ 0 & 0 & N_q^a & 0 & \text{-}N_r^a & 0 & 0 & 0 & N_q^b & 0 & N_r^b & 0 \\ 0 & 0 & 0 & N_1^a & 0 & 0 & 0 & 0 & 0 & N_1^b & 0 & 0 \\ 0 & 0 & 0 & 0 & N_1^a & 0 & 0 & 0 & 0 & 0 & N_1^b & 0 \\ 0 & 0 & 0 & 0 & 0 & N_1^a & 0 & 0 & 0 & 0 & 0 & N_1^b \end{bmatrix} \tag{3.8}$$

Where:

$$
\begin{aligned}
N_1^a(s) &= \frac{1}{2}(1-s) \\
N_q^a(s) &= \frac{1}{4}(2+s)(s-1)^2 \\
N_r^a(s) &= \frac{1}{8}L(1+s)(s-1)^2 \\
N_1^b(s) &= \frac{1}{2}(1+s) \\
N_q^b(s) &= -\frac{1}{4}(s-2)(1+s)^2 \\
N_r^b(s) &= -\frac{1}{8}L(s-1)(1+s)^2
\end{aligned}
$$

### 3.2.2 Calculation of equivalent damping matrix

Damping can be described as a mechanical phenomenon in which the system under motion dissipates energy which leads to decrease in system vibrations. The improvement in stiffness/mass ratio which is primarily achieved because of the reduction in mass and enhanced stiffness properties also lead to reduced damp-

ing and increased extension-shear coupling of the material. Hence, damping is an important parameter that should be considered in selection of material and designing any sort of vibration control for wind turbine. The damping matrix can be defined by the following equation [28]

$$D = 2G_D - D_a \tag{3.9}$$

Where, $G_D$ is the skew-symmetric matrix gyroscopic coupling matrix and can be defined in integral form as :

$$G_D = \int_L N_x^T \left( \int_A N_A^T \hat{\omega} N_A \rho dA \right) N_x dx \tag{3.10}$$

The skew-symmetric matrix gyroscopic coupling matrix is an inertial force matrix (due to rotating reference frame) directly proportional to the angular velocity. The detailed derivation of these forces also known as Coriolis forces can be found in reference [28, 68]. The skew-symmetric angular velocity matrix $\hat{\omega}$ can be defined as:

$$\hat{\omega} = \begin{bmatrix} 0 & -\omega_z & \omega_y \\ \omega_z & 0 & \omega_x \\ \omega_y & \omega_x & 0 \end{bmatrix}$$

Also, the aerodynamic damping matrix $D_a$ can be defined by the following equation

$$D_a = \int_L N_x^T T_a R_a A_D N_x dx \tag{3.11}$$

Where $T_a$ and $R_a$ are the transformation matrix for equivalent forces & moments and transformation matrix for rotation as given by Equations 3.12 and 3.13 respectively [69].

$$T_a = \begin{bmatrix} 1 & 0 & 0 \\ 0 & 1 & 0 \\ 0 & 0 & 1 \\ 0 & \text{-}d_z & d_y \\ d_z & 0 & 0 \\ \text{-}d_y & 0 & 0 \end{bmatrix} \tag{3.12}$$

$$R_a = \begin{bmatrix} 0 & 0 \\ \cos \alpha_U & \sin \alpha_U \\ \text{-}\sin \alpha_U & \cos \alpha_U \end{bmatrix} \tag{3.13}$$

$$A_D = \frac{1}{2} \rho_a C \frac{U^2}{U_D} \begin{bmatrix} 0 & -C'_L \cos(\beta) & C'_L \sin(\beta) & C'_L h & 0 & 0 \\ 0 & -C'_D \cos(\beta) & C'_D \sin(\beta) & C'_D h & 0 & 0 \end{bmatrix} \tag{3.14}$$

### 3.2.3   Equivalent Stiffness Matrix

The equivalent stiffness matrix $K$ can be defined in terms of elastic stiffness $(K_e)$, geometric element stiffness $(K_g)$, gyroscopic angular acceleration $(\dot{G})$, centrifugal stiffness $(C_K)$ and aerodynamic stiffness matrix $(K_a)$ as given in equation 3.15.

$$K = K_e + K_g + \dot{G} - C_K - K_a \tag{3.15}$$

48

The element stiffness matrix $K_e$ is defined in reference [70] in terms of the flexibility matrix $H$ and the elastic transformation matrix $T_e$ as given in equation 3.16.

$$K_e = T_e H^{-1} T_e^T \qquad (3.16)$$

The $T_e$ is the matrix for transforming internal forces on to the nodal forces and is defined in terms of distribution matrix $T_d$. The distribution Matrix $(T)$ can be defined in terms of normalized coordinates $\xi$ with domain $[-1, 1]$ as given in equation 3.18. The flexibility matrix $H$ is defined in terms of elements of cross-section flexibility matrix $C$ and its inverse namely cross-section stiffness matrix $K_{cs}$ is defined in equation 3.20.

$$T_e = \begin{bmatrix} -T_d(-1) \\ T_d(1) \end{bmatrix} \qquad (3.17)$$

$$T_d(\xi) = \begin{bmatrix} 1 & 0 & 0 & 0 & 0 & 0 \\ 0 & 1 & 0 & 0 & 0 & 0 \\ 0 & 0 & 1 & 0 & 0 & 0 \\ 0 & a\xi & 0 & 1 & 0 & 0 \\ -a\xi & 0 & 0 & 0 & 1 & 0 \\ 0 & 0 & 0 & 0 & 0 & 1 \end{bmatrix} \qquad (3.18)$$

49

$$H = 2a \begin{bmatrix} C_{11} + \frac{1}{3}a^2 C_{55} & C_{12} - \frac{1}{3}a^2 C_{54} & C_{13} & C_{14} & C_{15} & C_{16} \\ C_{21} - \frac{1}{3}a^2 C_{45} & C_{22} + \frac{1}{3}a^2 C_{44} & C_{13} & C_{14} & C_{15} & C_{16} \\ C_{31} & C_{32} & C_{33} & C_{34} & C_{35} & C_{36} \\ C_{41} & C_{42} & C_{43} & C_{44} & C_{45} & C_{46} \\ C_{51} & C_{52} & C_{53} & C_{54} & C_{55} & C_{56} \\ C_{61} & C_{62} & C_{63} & C_{64} & C_{65} & C_{66} \end{bmatrix} \tag{3.19}$$

$$K_{cs} = \begin{bmatrix} EA & 0 & 0 & 0 & 0 & 0 \\ 0 & K_{s2} G_S A & 0 & 0 & 0 & 0 \\ 0 & 0 & K_{s3} G_S A & 0 & 0 & 0 \\ 0 & 0 & 0 & G_S I^\rho & 0 & 0 \\ 0 & 0 & 0 & 0 & EI^\rho_{yy} & 0 \\ 0 & 0 & 0 & 0 & 0 & EI^\rho_{zz} \end{bmatrix} \tag{3.20}$$

Where $G_S$ is the shear modulus defined as $E/2(1 + v)$. The geometric stiffness matrix is defined in equation 3.21 in terms of longitudinal interpolation matrix $N_x$ and stress matrix $S$.

$$K_g = \int_L \begin{bmatrix} N_x^T & N_x'^{T} \end{bmatrix} S \begin{bmatrix} N_x \\ N_x' \end{bmatrix} dx \tag{3.21}$$

The stress matrix can be defined in terms of stress transformation matrix $\hat{T}_S$ and initial stress matrix $\hat{S}$ as given in equation 3.22. The variables $c_x$, $c_y$ and $c_z$ are the coordinates of the elastic center position vector while $a_x$, $a_y$ and $a_z$ are shear

center $(A_S)$ coordinates.

$$S = \begin{bmatrix} \hat{T}_{\hat{S}}^T & 0 \\ 0 & \hat{T}_{\hat{S}}^T \end{bmatrix} \hat{S} \begin{bmatrix} \hat{T}_S & 0 \\ 0 & \hat{T}_S \end{bmatrix} \tag{3.22}$$

$$\hat{T}_S = \begin{bmatrix} 1 & 0 & 0 & 0 & c_z & -c_y \\ 0 & 1 & 0 & -a_z & 0 & 0 \\ 0 & 0 & 1 & a_y & 0 & 0 \\ 0 & 0 & 0 & 1 & 0 & 0 \\ 0 & 0 & 0 & 0 & 1 & 0 \\ 0 & 0 & 0 & 0 & 0 & 1 \end{bmatrix} \tag{3.23}$$

The gyroscopic angular acceleration matrix $\dot{G}$ is derivative of gyroscopic coupling matrix defined in equation 3.10. The centrifugal stiffness matrix $C_K$ is defined in terms of longitudinal interpolation, area interpolation, skew symmetric angular velocity matrix and mass density in integration form.

$$\hat{S} = \begin{bmatrix} 0 & 0 & 0 & 0 & 0 & 0 & 0 & 0 & 0 & 0 & 0 & 0 \\ 0 & 0 & 0 & 0 & 0 & 0 & 0 & 0 & 0 & 0 & 0 & 0 \\ 0 & 0 & 0 & 0 & 0 & 0 & 0 & 0 & 0 & 0 & 0 & 0 \\ 0 & 0 & 0 & 0 & 0 & 0 & 0 & -Q_z^0 & Q_y^0 & a_zQ_z^0 + a_yQ_y^0 & 0 & 0 \\ 0 & 0 & 0 & 0 & 0 & 0 & 0 & 0 & 0 & 0 & 0 & 0 \\ 0 & 0 & 0 & 0 & 0 & 0 & 0 & 0 & 0 & 0 & 0 & 0 \\ 0 & 0 & 0 & 0 & 0 & 0 & 0 & 0 & 0 & 0 & 0 & 0 \\ 0 & 0 & 0 & 0 & 0 & 0 & 0 & Q_x^0 & 0 & -M_y^0 & 0 & 0 \\ 0 & 0 & a_zQ_z^0 + a_yQ_y^0 & Q_y^0 & -Q_z^0 & 0 & 0 & 0 & Q_x^0 & -M_z^0 & 0 & 0 \\ 0 & 0 & 0 & 0 & 0 & 0 & 0 & 0 & -M_z^0 & S^0 & 0 & 0 \\ 0 & 0 & 0 & 0 & 0 & 0 & 0 & 0 & -M_y^0 & 0 & 0 & 0 \\ 0 & 0 & 0 & 0 & 0 & 0 & 0 & 0 & 0 & 0 & 0 & 0 \end{bmatrix}$$

$$\tag{3.24}$$

$$C_K = \int_L N_x^T \left( \int_A N_A^T \hat{\omega}^T \hat{\omega} N_A \rho \, dA \right) N_x \, dx \tag{3.25}$$

The aerodynamic stiffness matrix uses sectional Lift and Drag values to calculate the effect of forces on stiffness as given in equation 3.26.

$$K_a = \int_L N_x^T T_a R_a A_K N_x \, dx \tag{3.26}$$

Where :

$$A_K = \frac{1}{2}\rho_a C U^2 \begin{bmatrix} 0 & 0 & 0 & C_L' & 0 & 0 \\ 0 & 0 & 0 & C_D' & 0 & 0 \end{bmatrix} \tag{3.27}$$

The equivalent force vector $f$ can be written in terms of centrifugal force $f_C$, angular acceleration force $f_G$, aerodynamic force $f_a$ and external force vector $f_e$ as given in equation 3.28

$$f = f_C - f_G + f_a + f_e \tag{3.28}$$

Where :

$$f_C = \int_L N_x^T \left( N_A^T \hat{\omega}^T \hat{\omega} x \rho dA \right) dx \tag{3.29}$$

$$f_G = \int_L N_x^T \left( N_A^T \hat{\alpha}^T x \rho dA \right) dx \tag{3.30}$$

$$f_a = \int_L N_x^T T_a R_a F_a dx \tag{3.31}$$

$$F_a = \frac{1}{2}\rho_a C U^2 (\alpha_U + \beta + \alpha_0) \begin{bmatrix} C_L' \\ C_D' \end{bmatrix} \tag{3.32}$$

Where:

$N_x(x)$ - Longitudinal Shape function

$T_a$ - Force and Moment transformation Matrix

$R_a$ - Rotational Transformation Matrix

$F_a$ - Aerodynamic Force Matrix due to rigid blade profile

$A_D$ - Aerodynamic force for damping due to blade deformation

$A_K$ - Aerodynamic force for stiffness due to transverse velocity of the blade

The closed form of these matrices are presented in Appendix of this report. The integral equations can be solved using numerical integration along the span of the blade using methods such as Gauss quadrature in a MATLAB code. This is in the process of development and once solved the results can be compared with the published results.

Aerodynamic model of wind turbine blades would contribute in making the forcing function, damping and stiffness term due to the deformation more realistic and would help determine the consequent change in inflow angle. A linearized dynamic stall model was obtained from reference [28] that accounts for all these terms. This aerodynamic model was studied and a brief description of this model along with equations is presented in this section. Generally, using the basic aerodynamic principle, lift is directly proportional to the relative angle of attack (AoA) $\alpha$ and relative wind velocity $U$ (Equation 3.33). The relative AoA was than subdivided in order to get separate terms for aerodynamic force, damping and stiffness matrix as given in Equation 3.34.

$$L_f \;=\; \frac{1}{2}\rho U^2 S_{ref}(C_{L_{\alpha_r}}\alpha_r + C_{L_0}) \qquad (3.33)$$

$$\alpha_r \;=\; \alpha_f + \alpha_K + \alpha_D \qquad (3.34)$$

The mean inflow angle $\alpha_f$ can be written in terms of mean wind flow angle ($\alpha_U$), twist angle ($\beta_t$), and profile camber ($\alpha_0$) contribution.

$$\alpha_f = \alpha_U - \beta_t + \alpha_0 \tag{3.35}$$

Where :

$$\tan \alpha_U = \frac{U_y}{U_z} \tag{3.36}$$

The contribution due to stiffness $\alpha_K$ can be written in terms of torsional degree of freedom $r_x$ and the damping contribution is given by equation 3.37.

$$\alpha_D = \frac{1}{U_D}(\dot{q}_z \sin \beta - \dot{q}_y \cos \beta + \dot{r}_x h) \tag{3.37}$$

Where:

$\rho$ - Air Density

$U$ - Relative Wind Velocity

$S_{ref}$ - Blade Reference Area

$\alpha_f$ - AoA for rigid blade profile

$\alpha_K$ - AoA due to blade deformation

$\alpha_D$ - AoA due to the velocity across blade profile

### 3.2.4  Rayleigh-Ritz Method

Principle of minimum potential energy at equilibrium position can be used to obtain natural frequencies. The natural frequencies of conservative systems may be obtained by equating the maximum kinetic energy to the maximum total potential energy associated with vibration. The detailed description of this method is given in [71] and briefly described here as follows:

- A displacement function of beam is assumed for the deflection curve consisting of series containing unknown parameters such as (n = 1, 2 ). The selected function needs to satisfy the geometric boundary conditions (Constraints pertaining to deflection & slopes) whereas the static boundary conditions needs not to fulfilled.

- Potential energy is than expressed in terms of unknown parameters $a_n$. As described earlier, using the fact that potential energy is minimum at equilibrium, we can get set of algebraic equations. These set of algebraic equations can be solved to get $a_n$ and subsequently potential energy can be obtained.

- $a_n$ is Substituted into assumed displacement function and approximate solution for natural frequencies and mode shapes can be obtained.

Rayleigh-Ritz method was developed on a basic principle that the overall energy of an enclosed system remains unchanged. The wind turbine can be considered as a largely conservative system and its natural frequencies will first be determined ignoring any losses due to aerodynamic and mechanical friction. Rayleigh-

Ritz Method was applied in order to obtain higher natural frequencies of wind turbine blade which was modelled as cantilever beam as shown in Figure 3.1. This method is highly influenced by assumed displacement shapes but at the same time allows to determine the higher frequencies of the turbine blades with more computational efficiency. The maximum displacement $f(x)$ in this method was assumed as the sum of the series of the weighing coefficient and assumed displacement functions. Natural frequencies were obtained for the different modes. The assumed displacement function, in this case must not have any discontinuity



Figure 3.1: A Simple cantilever beam with Length L

and should satisfy the geometric boundary conditions. i.e.

$$At \quad x = 0, \quad f = 0$$

$$At \quad x = 0, \quad f' = 0$$

Hence, the assumed displacement function for Rayleigh-Ritz method can be expressed in the general form:

$$f(x) = \sum_{i=1}^{n} W_i \phi_i \quad Where: \quad \phi_i = \left(\frac{x}{L}\right)^{i+1} \tag{3.38}$$

Where: $\quad W_i$ is the weighing coefficient.

Using the Rayleigh-Ritz concept, a MATLAB code for a uniform cantilever beam was implemented both for a third degree polynomial (Equation 3.39) and an infinite series solution for n degree polynomial (Equation 3.38). Polynomial assumed admissible Function [71]:

$$f(x) = W_1 \left(\frac{x}{L}\right)^2 + W_2 \left(\frac{x}{L}\right)^3 \tag{3.39}$$

Where:

$L$ - Length of the beam.

$W_1$ & $W_2$ - Weighing coefficients

Stiffness and mass matrix were obtained using Polynomial Admissible Functions, given in Equation 3.39, by differentiating Kinetic & Potential energy twice w.r.t weighing coefficients as shown in Equation 3.40 and 3.41.

$$K = \frac{\partial^2 V_m}{\partial W_i \partial W_j} \tag{3.40}$$

$$M = \frac{\partial^2 T_m}{\partial W_i \partial W_j} \tag{3.41}$$

Where:

$V_m$ - Potential Energy function

$T_m$ - Kinetic Energy function

The solution of an n degree polynomial was obtained through a MATLAB program which gives natural frequencies. The mass and stiffness matrix for an Infinite

Series Polynomial are given in reference [71] as:

$$K = \frac{(i+1)i(j+1)jEI}{(i+j-1)L^3} \tag{3.42}$$

$$M = \frac{mL}{(i+j+3)} \tag{3.43}$$

## 3.2.5   Implementation of FEM Matlab Code

In order to model the problem, the Finite Element technique can be used to obtain the mode shapes and natural frequencies. FEM is well-known technique and more complex problems, accommodating aerodynamic forcing function with three dimensional beam can be more easily modelled using this technique. As a test case for validation, the dimensions of the beam were taken from the literature [2] and a MATLAB routine was developed to obtain mode shapes and natural frequencies.

The geometric and material properties of the uniform cantilever beam are summarized in the form of a table 3.2.

| Characteristic | Value |
|---|---|
| Length | 2 m |
| Young Modulus | $21 \times 10^{10}$ Pa |
| Moment of Inertia | $60 \times 10^{-6}$ $kg.m^2$ |

Table 3.2: Geometric and Material properties for FEM analysis of beam [2]

The beam would be studied for forced vibration response once the forcing function is obtained. The MATLAB code was implemented for an isotropic, homogeneous beam with a constant value of young modulus and density. The beam was modelled consisting of two elements and the stiffness matrix for the individual

elements were obtained in the form of the matrix. Afterwards, the global stiffness matrix was assembled using the stiffness matrix of individual elements. The technique can be further developed for any number of elements to obtain mode shapes and natural frequencies. This is taken as a case of validation for the development of the complex beam code in order to apply the FEM on more complex problems later. The global stiffness matrix was obtained from the results as given below.

$$
K = \begin{bmatrix}
18900 & 18900 & -18900 & 18900 & 0 & 0 \\
18900 & 25200 & -18900 & 12600 & 0 & 0 \\
-18900 & -18900 & 37800 & 0 & -18900 & 18900 \\
18900 & 12600 & 0 & 50400 & -18900 & 12600 \\
0 & 0 & -18900 & -18900 & 18900 & -18900 \\
0 & 0 & 18900 & 12600 & -18900 & 25200
\end{bmatrix} N/m^2 \qquad (3.44)
$$

# CHAPTER 4

# AEROELASTIC MODELLING

## 4.1 Aerodynamics of Wind Turbine

The wind turbine rotor can be seen as a system of rotating beam-like structures. In order to estimate the forcing function, a three-dimensional formulation for beams in a rotating frame of reference is needed to be developed.

In a real time dynamic environment, the forcing function for wind turbine change as the aerodynamic forces oscillate. The objective is to obtain the forced response of the blade with more accurate representation of the aerodynamic loads. Hence, the challenge is to predict an appropriate model for forcing function $f(x,t)$. Aerodynamic force depends on the numerous parameters including blade profile, relative flow speed, stiffness and aerodynamic damping. All these parameters collectively determines the angle of attack or inflow angle which determine the lift and drag coefficient for a particular blade cross-section.

The governing equation 3.1 of vibration will accommodate the aerodynamic

force matrix and hence it will be able to predict the vibrations. The challenge faced by researchers is to find a suitable enough matrix which is very close in nature to the real time force changes on turbine blade and would also be valid for different blade cross-section and length. Also, the vibration mode should also include the vibrations effects of tower, nacelle and due to the rotation of the turbine itself.

First the vibration governing equation were studied with some background knowledge as it tells the exact nature of the aerodynamic matrix required. Also, it needs to be understood where we can accommodate the effects of the rotation of the turbine blade and what effect they have on aerodynamic force matrix or on governing equation 3.1. The aerodynamic theories that are applicable for aerodynamic calculation were studied. The literature survey suggests that the most popular theory for calculating aerodynamic load is Blade Element Momentum (BEM) Method and researchers used this theory for the development of an aerodynamic and mathematical model [16]. This is because BEM method has been found to be computationally efficient as compared to free wake vortex method. However, BEM based models have been found to be comparatively less accurate for predicting the aerodynamic force variations along the span of turbine blades. Therefore, there is a potential to improve current BEM models which would enable the researchers to make more accurate prediction of aerodynamic forces with relatively less computation time and cost. Moreover, there are some limitations of BEM theory and it is unable to predict accurate aerodynamic coefficients under

dynamic conditions such as during stall and rotor yaw.

On the other hand, vortex method predicts dynamic response with great accuracy and carries immense research potential. Infact, most researchers now focus on developing a reduced degree of freedom model based on vortex method which is also computationally efficient. There are numerous dynamic models including Beddoss-Leishman model, ONERA model and linearised airfoil flow model using Kirchoff flow theory. However, for this particular work, we used modified ONERA type model presented by Peters in [51]. This dynamic model was modified for wind turbine blades in order to obtain its sectional lift and drag which can be used in aeroelastic model. The ONERA type model has few advantages over other models which including the prediction of both lift and drag coefficient with a skewed cylindrical wake, finite number of states and absence of any hidden states among others.

## 4.2   Blade Element Momentum Model

Blade Element Momentum theory can be used to effectively calculate lift coefficient for a wind turbine. The flow over the wind turbine blades is shown in Figure 4.1

The basis for this theory is both Momentum and Blade Element Theory. Blade element theory is based on analysis of forces at a section of the blade, while momentum theory is based on conservation of momentum. It is assumed that

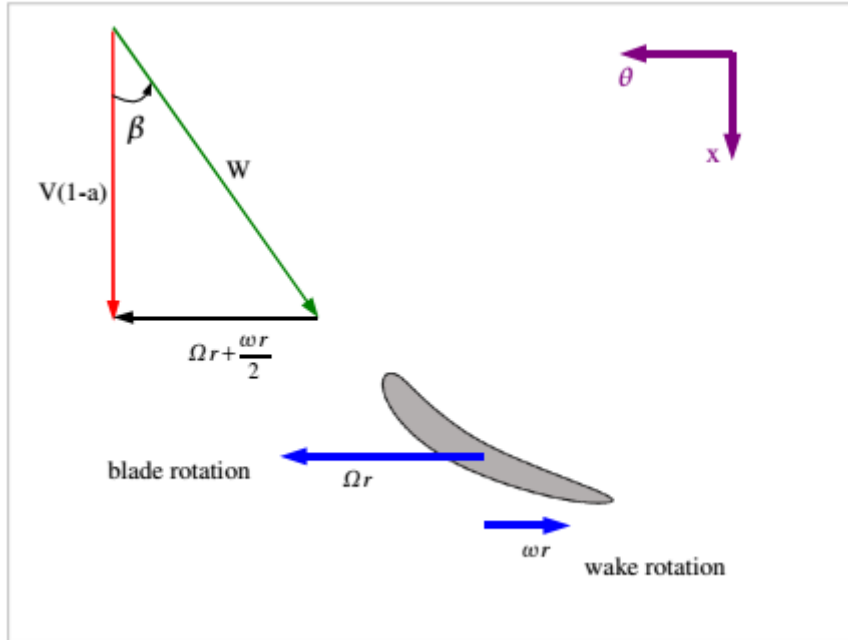- The aerodynamic interference between elements is negligible

Figure 4.1: The figure shows the flow over the wind turbine blade

- Airfoil shape contributes largely towards forces on the blades by altering its lift and drag characteristics.

Lift and drag forces act perpendicular and parallel, respectively, to relative wind. The relative wind is the vector sum of the wind velocity at the rotor, and the wind velocity due to rotation of the blade. The torque and force equations from momentum and blade element theory are equated along with some geometric relations to obtain an expression for lift coefficient. The method assumes that the airfoil section lift coefficient vs. angle of attack relation must be linear in the region of operation and the angle of attack must be small enough that the small-angle approximations can be used. This simplified method use an expression to find the angle of incidence of the relative wind at each blade element. The expressions

which are used to calculate the lift coefficient are given below as :

$$Lift\ Curve\ Equation : C_L = C_{L,0} + C_{L,\alpha}\alpha \tag{4.1}$$

$$Solidity : \sigma_S = \frac{Bc}{2\pi R} \tag{4.2}$$

$$Tip\ Speed\ Ratio : \lambda = \frac{\omega r}{U} \tag{4.3}$$

$$Local\ Speed\ Ratio : \lambda_r = \frac{\lambda r}{R} \tag{4.4}$$

$$Relative\ Flow\ Angle : \beta_r = 90° - \frac{2}{3}\tan^{-1}\left(\frac{1}{\lambda_r}\right) \tag{4.5}$$

$$Incidence\ Angle : i = \beta_t - \beta_r \tag{4.6}$$

$$Axial\ Factor : a = \left(1 + \frac{4cos^2(\beta)}{\acute{o}C_L sin(\beta)}\right)^{-1} \tag{4.7}$$

$$Angular\ Induction\ Factor\ \acute{a} = \frac{1 - 3a}{4a - 1} \tag{4.8}$$

$$Geometric\ Relation : tan(\beta_r) = \lambda_r\frac{1 + \acute{a}}{1 - a} \tag{4.9}$$

$$Angular\ Factor = \left[\frac{\acute{o}C_L}{4\lambda_r cos(\beta_r)}\right](1 - a) \tag{4.10}$$

However, the solution for the lift coefficient cannot be found directly from the equations but an iterative process is adopted. For the initial analysis, The drag coefficient $C_D$ is assumed to be zero while the tip loss correction factor Q is assumed to be one. The step by step procedure is outlined below:

1. Find the value of Solidity using the equation 4.2 .

2. Find the Relative flow angle using the equation 4.5 .

3. From the blade geometry, use the corresponding twist angle to find the section incidence angle $i$ using equation 4.6 .

65

4. Find the initial guess for axial induction factor $a$ and angular induction factor $á$ using equations 4.7 and 4.8 respectively.

5. Use values of $a$ and $á$ obtained in step 4 to find the value of $\beta_r$ using geometric relation given in equation 4.9

6. Calculate the incidence angle using equation 4.6 by using the corresponding value of twist angle $\beta_t$ from given blade geometry.

7. Use the value of $\beta_t$ obtained in step 6 to find the value of $C_L$ using the equation 4.1 from $C_L$ vs $\alpha$ curve.

8. Find the new values for axial induction factor $a$ and angular induction factor $á$ using equations 4.7 and 4.10 respectively.

9. Repeat the procedure from Step 5 to 8 until the difference between the new value of axial and angular induction factors are very close together (i.e. $\Delta a$ and $\Delta á <= 0.0001$)

## 4.3   Dynamic Aeroelastic Model

The rotor aeroelasticity is a coupled problem and it involves coupling between different modules such as structure and aerodynamics. This modified aeroelastic model, initially known as Peters-He Model, was developed by Peters and Su and includes structural-dynamic model, induced flow model along with the airloads model. The aerodynamics and airfoil effects is based on a ONERA type model and

the integration of structural-dynamics with airloads allow this model to include the past history of blade motions. This model was used to calculate the lift and drag coefficient of the turbine blade section under wake conditions. The lift and drag coefficients are defined by the equations 4.12 and 4.12:

$$C_l = \frac{L_y}{\rho b U^2} \tag{4.11}$$

$$C_d = \frac{L_x}{\rho b U^2} \tag{4.12}$$

Moreover, the lift and drag are defined in reference and are given in equation 4.13 as below:

$$L_y = \rho 2\pi b u_0 (w_0 - \lambda_0 + \frac{1}{2}w_1)$$

$$L_x = -\rho 2\pi b (w_0 - \lambda_0) + (w_0 - \lambda_0 + \frac{1}{2}w_1) \tag{4.13}$$

The coefficients $w_0$ and $w_1$ represents Fourier coefficients and are explicitly defined in reference for NACA 4 digit airfoil through an empirical relation in equation 4.14. Also, the induced flow $\lambda_0$, which is defined in the model using the equation 4.15, can be written in Fourier form in terms of shape functions and inflow expansion coefficients :

$$w_0 = \frac{q}{(1-q^2)^2} \left[ \frac{4}{\pi} \{ q \sin^{-1}(q) + \sqrt{(1+q^2)} \} - (1+q^2) \right] 4m$$

$$w_1 = \frac{1}{(1-q^2)^2} \left[ (1+q^2) - \frac{4}{\pi} q \{ \sin^{-1}(q) + q\sqrt{1+q^2} \} \right] 4m \tag{4.14}$$

$$\lambda_0 = \sum_{r,j} \bar{\phi}_j^r J_0(r\hat{b}) \Omega R [\alpha_j^r \cos(r\psi_q) + \beta_j^r \sin(r\psi_q)] \tag{4.15}$$

For NACA 0012 airfoil, the typical values of $w_0$ and $w_1$ are 0.20 and 0.10

as noted in reference and more recently these values were published in another reference for 18 different NACA airfoils. The term $\phi_j^r$ basically represent expansion functions and are simple polynomials in $\bar{r}$ and can be obtained by solving series given in reference. The m and n are harmonic numbers and they follow a certain convention for cosine and sine terms such that for cosine coefficients $m = 0, 1, 2, 3, ...$ and $n = 1, 3, 5, ..$ while for sine coefficients $m = 1, 2, 3, ...$ and $n = 2, 4, 6, ...$ The r and j also follow a similar convention as m and n and an example is given for $\phi$ vector for both cosine and sine terms in equation 4.16.

$$
\phi_j^r = \begin{pmatrix} \phi_1^0 \\ \phi_3^1 \\ \phi_5^2 \\ \phi_7^3 \end{pmatrix}, \quad \phi_j^r = \begin{pmatrix} \phi_2^1 \\ \phi_4^2 \\ \phi_6^3 \\ \phi_8^4 \end{pmatrix} \tag{4.16}
$$

The term $J_0$ represents Beseel function of first kind can be obtained from a simplified form of the Bessel functions $J_0(r\hat{b})$ as represented through equation 4.17. The angle $\psi_q$ is the azimuth angle given by equation 4.18 in which $q$ represents the number of $q^{th}$ blade. The $\alpha_n^m$ and $\beta_n^m$ are the cosine and sine inflow expansion coefficients both of which can be calculated by solving first order differential equations 4.20 given below in matrix form.

$$
J_0(r\hat{b}) = \sum_{r=0}^{\infty} (-1)^r \frac{1}{r!(n+r)!} \left(\frac{x}{2}\right)^{2r+n} \tag{4.17}
$$

$$
\psi_q = \omega t + \frac{2}{3}\pi(q-1) \tag{4.18}
$$

68

$$\phi_j^r = \frac{1}{2}\sqrt{(2n+1)\pi} \sum_{q=m,m+2}^{n-1} \bar{r}^q \frac{(-1)^{\frac{(q-m)}{2}}(n+q)!!}{(q-m)!!(q+m)!!(n-q-1)!!} \qquad (4.19)$$

$$\{\alpha_n^m\}^* + [\bar{L}^c]^{-1}[V_n^m]\{\alpha_n^m\} = \{\tau_n^{mc}\}$$

$$\{\beta_n^m\}^* + [\bar{L}^s]^{-1}[V_n^m]\{\beta_n^m\} = \{\tau_n^{ms}\} \qquad (4.20)$$

The solution of the differential equation requires determination of all the matrices including mass flow matrix $(V_n^m)$, influence coefficient matrices ($\bar{L}^c$ and $\bar{L}^s$) and forcing vectors ($\tau_n^{mc}$ and $\tau_n^{ms}$) . The mass flow matrix is a diagonal matrix and its each element is equal to free stream velocity for the case of wind turbine blades. This is a reasonable assumption because in case of wind turbine blades, as opposed to a helicopter blades, there is no energy added to the flow from the rotor. The sine and cosine influence coefficients can be written in terms of wake skew angle and azimuthal harmonics as given in reference in terms of elements of matrix $L_{jn}^{rm}$. An example is given for cosine matrix $\bar{L}^c$ in equation 6.12, where j and n are row-column pair within each r and m row-column division. In order to find forcing vectors, a reasonable estimate of the lift distribution is required which can be obtained through equation 4.22 .

$$\bar{L}^c = \left( \begin{array}{cc|cc} L_{11}^{00} & L_{13}^{00} & L_{12}^{01} & L_{14}^{01} \\ \\ L_{31}^{00} & L_{33}^{00} & L_{32}^{01} & L_{34}^{01} \\ \hline \\ L_{21}^{10} & L_{23}^{10} & L_{22}^{11} & L_{24}^{11} \\ \\ L_{41}^{10} & L_{43}^{10} & L_{42}^{11} & L_{44}^{11} \end{array} \right) \qquad (4.21)$$

$$L_s = \rho C_{L\alpha} b u_0 (w_0 - \lambda_0) + \rho \delta b u_0 w_1 \qquad (4.22)$$

69

In equation 4.22, the $\delta$ is defined as the pitch rate coefficient which can be assumed to be equal to $\pi$ for a thin airfoil while $u_0$ is a Fourier coefficient obtained by equation 4.23 in which $u$ represents the component of the flow parallel to the airfoil. The term $u_0$ is the Fourier expansion coefficient which can be obtained from the component of flow parallel to the airfoil ($u$) as given by equation 4.23.

$$u_0 = \frac{1}{\pi} \int_a^b u d\theta \tag{4.23}$$

The forcing vectors can then be obtained by evaluating Fourier coefficients which are given in series form in terms of lift, azimuth angle, Bessel function and expansion functions in reference. An example is given for for both cosine and sine forcing vector $T_n^{mc}$ in equation 4.24, where m and n follows the same convention as described before.

$$\tau_n^{mc} = \begin{pmatrix} \tau_1^{0c} \\ \tau_3^{1c} \\ \tau_5^{2c} \\ \tau_7^{3c} \end{pmatrix}, \quad \tau_n^{ms} = \begin{pmatrix} \tau_2^{1s} \\ \tau_4^{2s} \\ \tau_6^{3c} \\ \tau_8^{4c} \end{pmatrix} \tag{4.24}$$

Similarly, the $\alpha_n^m$ and $\beta_n^m$ vectors can be defined in the similar manner. The initial conditions for both $\alpha$ and $\beta$ were assumed to be zero as an initial guess as

defined in 4.25.

$$\alpha_n^m = \begin{pmatrix} \alpha_1^0 \\ \alpha_3^1 \\ \alpha_5^2 \\ \alpha_7^3 \end{pmatrix}, \quad \beta_n^m = \begin{pmatrix} \beta_2^1 \\ \beta_4^2 \\ \beta_6^3 \\ \beta_8^4 \end{pmatrix} \tag{4.25}$$

Using these initial conditions, the first order differential equations 4.20 can be solved numerically using any standard method such as Runge-Kutta 4th order. However, there is a coupling between lift and the inflow model as can be observed from equation 4.22 and 4.15. Therefore, the forcing vectors must be updated after every solution of differential equation using the lift term (equation 4.22) which in turn should be updated by the induced flow term (equation 4.15).

### 4.3.1 Solution Strategy

The dynamic aeroelastic model was obtained through numerical solution of first order differential equation and the adopted approach is summarized in the form of a flow chart as shown in Figure 4.2.

The initial conditions are obtained from atmospheric and geometric conditions.

## 4.4 Verification of Aeroelastic Model

The model is based on Theodorsen function which can be evaluated in terms of Bessel functions of the first and second kind. One practical approximation for rotorcraft applications having small frequencies consists of real and imaginary
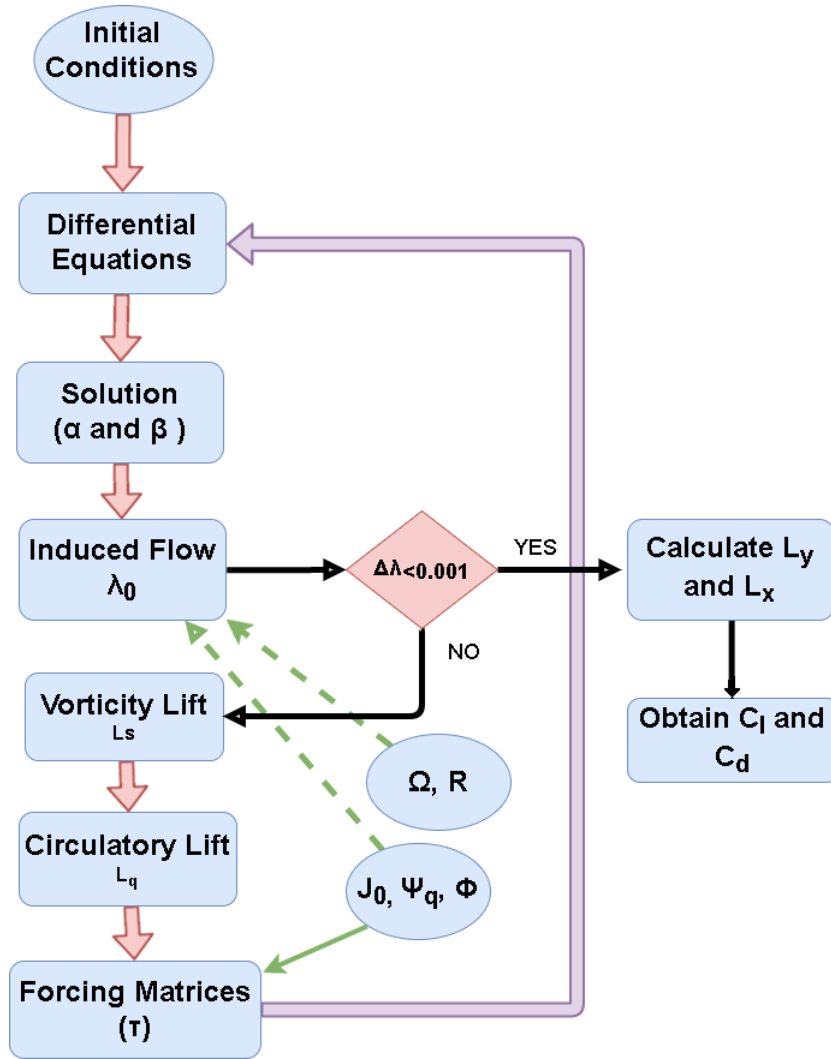
71

Figure 4.2: The Flow chart presents a summary for solving dynamic Aeroelastic Model

part and can be given by

$$C(k) \approx \left(1 - \frac{\pi}{2}k\right) + \iota k \left(\ln \frac{k}{2} + \gamma_e\right) \tag{4.26}$$

Where:

$$\gamma_e = 0.5772156 \quad (EulerConstant)$$

$$\omega_k = \frac{\omega b}{U} \quad (ReducedFrequency)$$

In case of wind turbine blades, whose aspect ratio is usually more than 7, the reduced frequency can be estimated as $0.05n$.

# CHAPTER 5

# CONTROLLER DESIGN

In this chapter, the Optimal LQR control technique and its effects on the active control of wind turbine blade vibrations have been discussed. A MATLAB code was developed to design the LQR controller and to study the response of wind turbine blade model to various disturbance input types. The aim is to design a responsive high-performance controller for a flexible wind turbine blade subjected to time varying loads. The wind turbine model can have infinite number of modes, however, the controller would only focus on the most significant modes in order to avoid complexity and wastage of control effort [27].

## 5.1   Linear Quadratic Regulator

We will consider a system represented with a state space model having a control input represented by $u(t)$ and a disturbance input represented by r(t) as given by equation 5.1.

$$\dot{x} = Ax(t) + Bu(t) + Er(t) \tag{5.1}$$

The state space equation can be remodelled by substituting the control input $u(t)$ with control gain row vector and state column vector $x(t)$. The control gains $(g_1, g_2, g_3, g_4...)$ can be varied to achieve desirable performance of the controlled response. The derivation steps to remodel the state space equation are summarized below:

Let:

$$u(t) = -gx(t) \tag{5.2}$$

Substituting the above form of control input into the state space equation 5.1 and the result can be rearranged to obtain the desired form.

$$\dot{x} = Ax(t) + B(-gx(t)) + Er(t)$$

$$\dot{x} = (A - Bg)x(t) + Er(t)$$

$$\dot{x} = A_c x(t) + Er(t)$$

Where:

$$A_c = A - Bg$$

In LQR control, the feedback gain $g$ is selected as to minimize the quadratic

function which is given by:

$$J = \frac{1}{2}\int_0^\infty (x^T(t)Qx(t) + u^T(t)Ru(t))dt \tag{5.3}$$

In the above equation, $Q$ represents the weighing matrix of state variables $x$ while the $R$ represents the weighing matrix of input variables $u$. Generally, $Q$ is selected as a substantial sized value for more prompt response while a larger value of $R$ increases the energy consumption of the controller. Moreover, the feedback gain also depends on the two weighing matrix $Q$ and $R$ and is calculated using the equation 5.4. There are numerous techniques for obtaining Q and R, however, it can be selected by trial and error for initial analysis.

$$g = R^{-1}B^T P \tag{5.4}$$

In the above equation, $P$ is the symmetric positive solution of Riccati equation given by the equation below:

$$PA + A^T P + Q - PBR^{-1}B^T P = 0 \tag{5.5}$$

# CHAPTER 6

# RESULTS AND DISCUSSION

The main aim of this study is to reduce edgewise vibrations using an aeroelastic model of a wind turbine blade. The active vibration control of a wind turbine aeroelastic model was carried out in numerous stages. First, the Rayleigh-Ritz and blade element momentum model was studied and a comparison was made between the results obtained from MATLAB routine and published experimental data. The BEM results signifies the need of an alternate aeroelastic model and depict the inaccuracy of analytical results at various tip speed ratios ($\lambda$ ). In the next section, results from an induced flow based model along with the various matrices are outlined. The NACA 0012 airfoil was used for evaluation of these matrices and induced flow results. Finally, the system response and controlled response results are presented with validation.

## 6.1 Results of Rayleigh Ritz Method

The results for uniform cantilever beam from Rayleigh Ritz method, as described in section 3.2.4, were compared with the existing experimental and numerical work and were found to be in agreement with the published data. The table 6.1 summarizes the results for both the third order and the infinite series polynomial. The results depict that the second and third modes are more closer to experimental results than the results obtained using FEM analysis method by [1]. However, the admissible polynomial being used in this case is unable to capture the first modal frequency. Hence it is suggested to use various admissible functions as a future work to capture maximum modal frequencies in range. [1]

| Mode | Experiment [1] | FEM [1] | Rayleigh-Ritz | | % Difference |
|------|----------------|---------|---------------|-----------|--------------|
| | | | 3rd Order | nth order | |
| 2 | 13.64 | 14.42 | 13.6179 | 13.5856 | 0.4 |
| 3 | 36.64 | 40.40 | 42.7451 | 34.0099 | 7.17 |

Table 6.1: Comparison of natural frequencies of Uniform Cantilever beam (Rayleigh-Ritz Method)

## 6.2 BEM Model Results

In this section, the BEM method was used to obtain the Power Coefficient of a wind turbine blade using a Matlab routine named "BladeElement.m". A comparison of the coefficient was made with published data for wind turbine blades. The geometric profile of wind turbine blade was obtained from an illustrated graph of a turbine blade and has been summarized in the form of a table 6.2.

| Blade Radius [m] | Chord Length [m] | Twist Angle [°] |
|---|---|---|
| 0.05 | 0.030 | 37 |
| 0.10 | 0.080 | 28 |
| 0.15 | 0.060 | 19 |
| 0.20 | 0.050 | 13 |
| 0.25 | 0.045 | 9.5 |
| 0.30 | 0.040 | 7.0 |
| 0.35 | 0.035 | 5.0 |
| 0.40 | 0.030 | 2.5 |
| 0.45 | 0.025 | -1.0 |

Table 6.2: Geometric properties of Wind Turbine Blade [3]

The airfoil used for this comparative study was NREL s286 as shown in Figure 6.1 and its lift and drag curve equations were obtained through curve fitting in MATLAB using the best-fit Xfoil software results from reference [3].
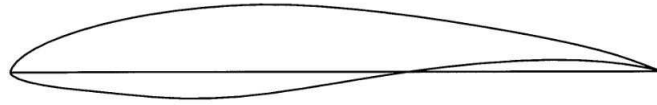


Figure 6.1: The figure shows the shape of the NREL s286 airfoil

Equation for lift and drag curves:

$$C_l = 1.7 \times 10^{-5}\alpha^4 - 3.7 \times 10^{-4}\alpha^3 + 2.4 \times 10^{-3}\alpha^2 + 0.12\alpha + 0.5 \qquad (6.1)$$

$$C_d = 2.3 \times 10^{-6}\alpha^4 - 1 \times 10^{-5}\alpha^3 + 4.2 \times 10^{-5}\alpha^2 + 0.00055\alpha + 0.021 \qquad (6.2)$$

The data presented here is for a small-scaled wind turbine which was specifically manufactured for wind tunnel testing. The simple blade element model was used for aerodynamic analysis in MATLAB while the published experimental results of Power coefficient ($C_P$) and Thrust Coefficient ($C_T$) were extracted from

reference [3]. These coefficients were analytically calculated using BEM theory along with equation 6.3 and 6.4.

$$Power\,Coefficient : C_P = \frac{\omega M}{\frac{1}{2}\rho U_\infty^3 A} \tag{6.3}$$

$$Thrust\,Coefficient : C_T = \frac{T}{\frac{1}{2}\rho U_\infty^2 A} \tag{6.4}$$

The value of tip speed ratio ($\lambda$) was varied while all the other geometric and dynamic parameters including the wind turbine airfoil, rotational velocity, wind speed, etc were kept same and are summarized in the form of a table. In this study, a higher value ($10m/s$) of wind speed was used, however, local meteorological data obtained from various published resources shows that the wind speed varies between 4 to 8 $m/s$ [12, 13].

| Parameters | Values |
|---|---|
| Rotational Velocity | 7 rad/s |
| Airfoil Type | NREL s826 |
| $N_{crit}$ | 3.0 |
| Wind speed | 10 m/s |
| Reynolds Number | $1 \times 10^5$ |

Table 6.3: Input parameters for Wind Turbine Blade [3]

The lift and drag forces were compared and the difference between experimental and analytical results are summarized in the form of table 6.4. It is clear from table that there is a substantial error for higher and lower values of $\lambda$ and hence a better aerodynamic model is required in order to improved the performance calculation for a wind turbine. The model should take into account the vorticity and other turbulent effects such as those accounted for in the vortex method.

| $\lambda$ | Experimental | BEM | % Difference |
|---|---|---|---|
| 2 | 0.05 | 0.04 | 20 |
| 3 | 0.14 | 0.10 | 29 |
| 4 | 0.39 | 0.32 | 18 |
| 5 | 0.46 | 0.42 | 8.7 |
| 6 | 0.49 | 0.45 | 8.1 |
| 7 | 0.48 | 0.44 | 8.3 |
| 8 | 0.41 | 0.42 | 2.4 |
| 9 | 0.32 | 0.37 | 15.6 |
| 10 | 0.20 | 0.31 | 55 |

Table 6.4: Comparison of Power Coefficient of a Wind Turbine Blade [3]

## 6.3    Dynamic Model Results

The matrices obtained are as follows:

$$
\bar{L}^c =
\begin{bmatrix}
0.4775 & 0.0810 & -0.1045 & 0 \\
0.0810 & 0.1857 & -0.0684 & -0.0510 \\
0.2089 & 0.1368 & 0 & 0 \\
0 & 0.1019 & 0 & 0
\end{bmatrix}
\tag{6.5}
$$

$$
\bar{L}^s =
\begin{bmatrix}
0 & 0 & -0.0796 & 0 \\
0 & 0 & -0.0593 & -0.0473 \\
0.0796 & 0.0593 & 0 & 0 \\
0 & 0.0473 & 0 & 0
\end{bmatrix}
\tag{6.6}
$$

$$
\bar{V}_n^m =
\begin{bmatrix}
15 & 0 & 0 & 0 \\
0 & 15 & 0 & 0 \\
0 & 0 & 15 & 0 \\
0 & 0 & 0 & 15
\end{bmatrix}
\tag{6.7}
$$

81

$$\phi_j^{rc} = \begin{pmatrix} -1.5 \\ -0.052\bar{r^2} - 0.39 \\ -3.2 \times 10^{-5}\bar{r^4} - 1.7 \times 10^{-3}\bar{r^2} - 0.012 \\ -9.0 \times 10^{-9}\bar{r^6} - 1.6 \times 10^{-6}\bar{r^4} - 3.0 \times 10^{-5}\bar{r^2} - 2.3 \times 10^{-4} \end{pmatrix} \quad (6.8)$$

$$\phi_j^{rs} = \begin{pmatrix} -0.99 \\ -6.9 \times 10^{-3}\bar{r^2} - 0.055 \\ 0 \\ 0 \end{pmatrix} \quad (6.9)$$

$$\tau_n^{mc} = \begin{pmatrix} 17.0000 \\ -8.3000 \\ 0.1800 \\ -0.0013 \end{pmatrix}, \quad \tau_n^{ms} = \begin{pmatrix} 17.0000 \\ -1.3000 \\ 0 \\ 0 \end{pmatrix} \quad (6.10)$$

$$\bar{L}^c = \begin{pmatrix} L_{11}^{00} & L_{13}^{00} & L_{12}^{01} & L_{14}^{01} & L_{13}^{02} & L_{15}^{02} & L_{14}^{03} & L_{16}^{03} & L_{15}^{04} & L_{17}^{04} \\[4pt] L_{31}^{00} & L_{33}^{00} & L_{32}^{01} & L_{34}^{01} & L_{33}^{02} & L_{35}^{02} & L_{34}^{03} & L_{36}^{03} & L_{35}^{04} & L_{37}^{04} \\[4pt] L_{21}^{10} & L_{23}^{10} & L_{22}^{11} & L_{24}^{11} & L_{23}^{12} & L_{25}^{12} & L_{24}^{13} & L_{26}^{13} & L_{25}^{14} & L_{27}^{14} \\[4pt] L_{41}^{10} & L_{43}^{10} & L_{42}^{11} & L_{44}^{11} & L_{43}^{12} & L_{45}^{12} & L_{44}^{13} & L_{46}^{13} & L_{45}^{14} & L_{47}^{14} \\[4pt] L_{31}^{20} & L_{33}^{20} & L_{32}^{21} & L_{34}^{21} & L_{33}^{22} & L_{35}^{22} & L_{34}^{23} & L_{36}^{23} & L_{35}^{24} & L_{37}^{24} \\[4pt] L_{51}^{20} & L_{53}^{20} & L_{52}^{21} & L_{54}^{21} & L_{53}^{22} & L_{55}^{22} & L_{54}^{23} & L_{56}^{23} & L_{55}^{24} & L_{57}^{24} \\[4pt] L_{41}^{30} & L_{43}^{30} & L_{42}^{31} & L_{44}^{31} & L_{43}^{32} & L_{45}^{32} & L_{44}^{33} & L_{46}^{33} & L_{45}^{34} & L_{47}^{34} \\[4pt] L_{61}^{30} & L_{63}^{30} & L_{62}^{31} & L_{64}^{31} & L_{63}^{32} & L_{65}^{32} & L_{64}^{33} & L_{66}^{33} & L_{65}^{34} & L_{67}^{34} \\[4pt] L_{51}^{40} & L_{53}^{40} & L_{52}^{41} & L_{54}^{41} & L_{53}^{42} & L_{55}^{42} & L_{54}^{43} & L_{56}^{43} & L_{55}^{44} & L_{57}^{44} \\[4pt] L_{71}^{40} & L_{73}^{40} & L_{72}^{41} & L_{74}^{41} & L_{73}^{42} & L_{75}^{42} & L_{74}^{43} & L_{76}^{43} & L_{75}^{34} & L_{77}^{44} \end{pmatrix} \tag{6.11}$$

$$\bar{L}^s = \begin{pmatrix} L_{22}^{11} & L_{24}^{11} & L_{23}^{12} & L_{25}^{12} & L_{24}^{13} & L_{26}^{13} & L_{25}^{14} & L_{27}^{14} \\[4pt] L_{42}^{11} & L_{44}^{11} & L_{43}^{12} & L_{45}^{12} & L_{44}^{13} & L_{46}^{13} & L_{45}^{14} & L_{47}^{14} \\[4pt] L_{32}^{21} & L_{34}^{21} & L_{33}^{22} & L_{35}^{22} & L_{34}^{23} & L_{36}^{23} & L_{35}^{24} & L_{37}^{24} \\[4pt] L_{52}^{21} & L_{54}^{21} & L_{53}^{22} & L_{55}^{22} & L_{54}^{23} & L_{56}^{23} & L_{55}^{24} & L_{57}^{24} \\[4pt] L_{42}^{31} & L_{44}^{31} & L_{43}^{32} & L_{45}^{32} & L_{44}^{33} & L_{46}^{33} & L_{45}^{34} & L_{47}^{34} \\[4pt] L_{62}^{31} & L_{64}^{31} & L_{63}^{32} & L_{65}^{32} & L_{64}^{33} & L_{66}^{33} & L_{65}^{34} & L_{67}^{34} \\[4pt] L_{52}^{41} & L_{54}^{41} & L_{53}^{42} & L_{55}^{42} & L_{54}^{43} & L_{56}^{43} & L_{55}^{44} & L_{57}^{44} \\[4pt] L_{72}^{41} & L_{74}^{41} & L_{73}^{42} & L_{75}^{42} & L_{74}^{43} & L_{76}^{43} & L_{75}^{34} & L_{77}^{44} \end{pmatrix} \tag{6.12}$$

These matrices were used to solve the differential equation and obtain cosine and sine inflow expansion coefficients. These coefficients were then used to calculate

the induced flow as defined earlier. Also, the result of differential equation was obtained and compared with the published results of the model. The results of ONERA type model were subsequently used to obtain stiffness and damping matrix along with forcing vector of state space form of Euler Bernoulli equation.

## 6.4   Validation of Stiffness Matrix

In order to validate the simplified form of mass matrix, a space frame element which had same DOF was taken and compared with the result obtained from MATLAB routine [72]. The mass matrix was found to be in agreement with that obtained from result and is shown below:
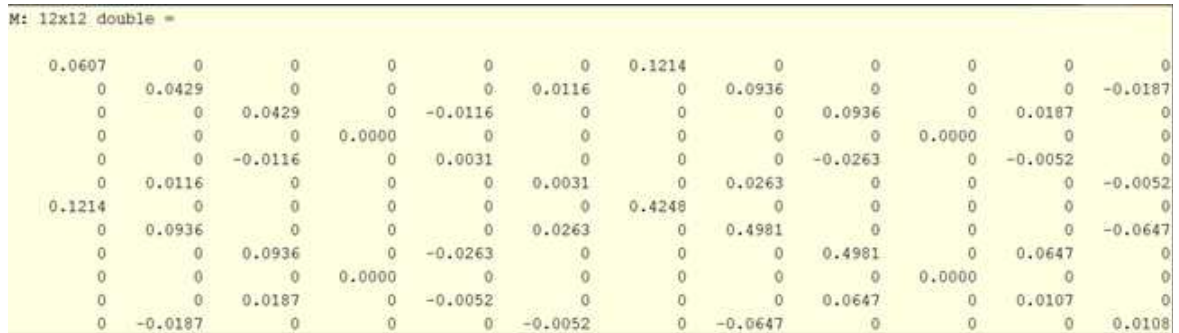
```
M: 12x12 double =

  0.0607        0        0        0        0        0   0.1214        0        0        0        0        0
       0   0.0429        0        0        0   0.0116        0   0.0936        0        0        0  -0.0187
       0        0   0.0429        0  -0.0116        0        0        0   0.0936        0   0.0187        0
       0        0        0   0.0000        0        0        0        0        0   0.0000        0        0
       0        0  -0.0116        0   0.0031        0        0        0  -0.0263        0  -0.0052        0
       0   0.0116        0        0        0   0.0031        0   0.0263        0        0        0  -0.0052
  0.1214        0        0        0        0        0   0.4248        0        0        0        0        0
       0   0.0936        0        0        0   0.0263        0   0.4981        0        0        0  -0.0647
       0        0   0.0936        0  -0.0263        0        0        0   0.4981        0   0.0647        0
       0        0        0   0.0000        0        0        0        0        0   0.0000        0        0
       0        0   0.0187        0  -0.0052        0        0        0   0.0647        0   0.0107        0
       0  -0.0187        0        0        0  -0.0052        0  -0.0647        0        0        0   0.0108
```

Figure 6.2: The figure shows the mass matrix for 12 DOF, six deflections and six rotations

## 6.5 LQR Control Response

The LQR control response was obtained using a MATLAB routine and the results are summarized in the form of the time response. The state space model was obtained using and is given below.

$$\lambda_{1,2} = 0.0371, -0.0381 \quad and \quad \lambda_{3,4} = -4.3989 \pm 8.2842i$$

The system is given below:

$$A = \begin{bmatrix} 0 & 0 & 1 & 0 \\ 0 & 0 & 0 & 1 \\ 0.0014 & -1.8022 \times 10^{-5} & -9.9986 \times 10^{-4} & -1.8022 \times 10^{-9} \\ -6.7892 \times 10^{-10} & -8.7978 \times 10^{10} & -6.7892 \times 10^{-14} & -8.7978 \times 10^{3} \end{bmatrix}$$

$$B = \begin{bmatrix} 0 \\ 0 \\ -0.0058 \\ -3.5684 \times 10^{8} \end{bmatrix}, \quad C = \begin{bmatrix} 0 & 0 & 0.7597 & 0.6316 \end{bmatrix}, \quad D = \begin{bmatrix} 0 \end{bmatrix}, \quad E = \begin{bmatrix} 0 \\ 0 \\ 1.3708 \times 10^{3} \\ 5.1175 \times 10^{-11} \end{bmatrix}$$
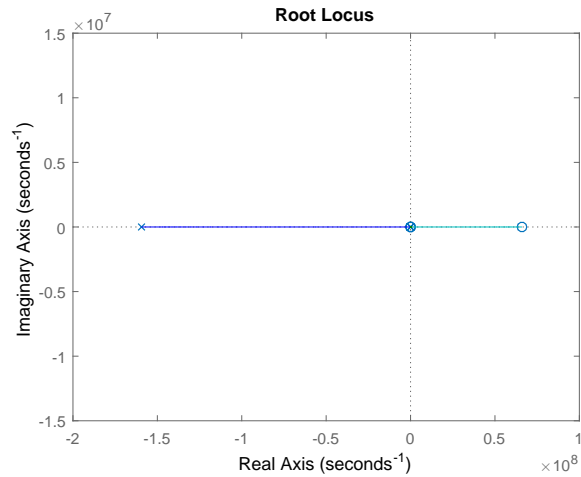
Figure 6.3: The figure shows the root locus for the system
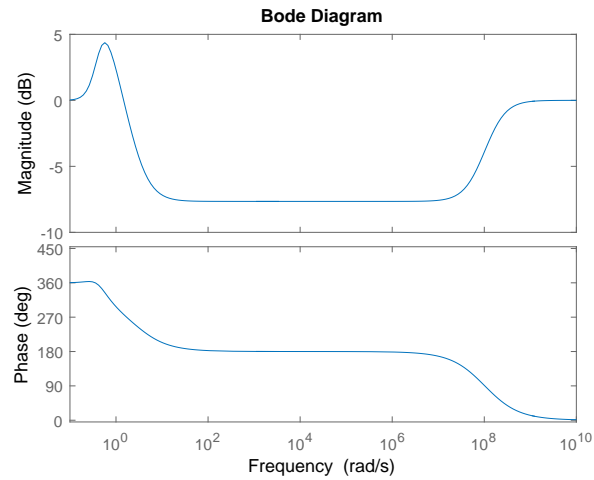


Figure 6.4: The figure shows the bode plot for the system

## 6.6   The Effect of variation of Young Modulus

The young modulus was varied from 69 to $150N/m^2$. The results are presented
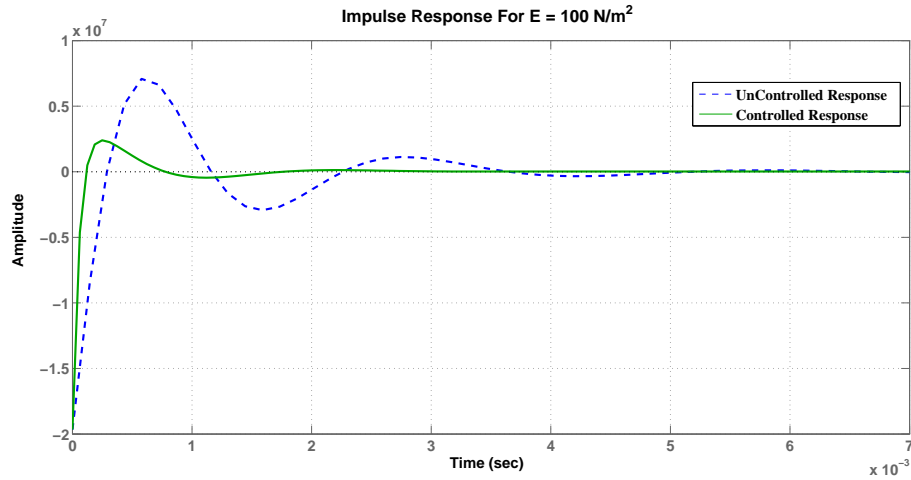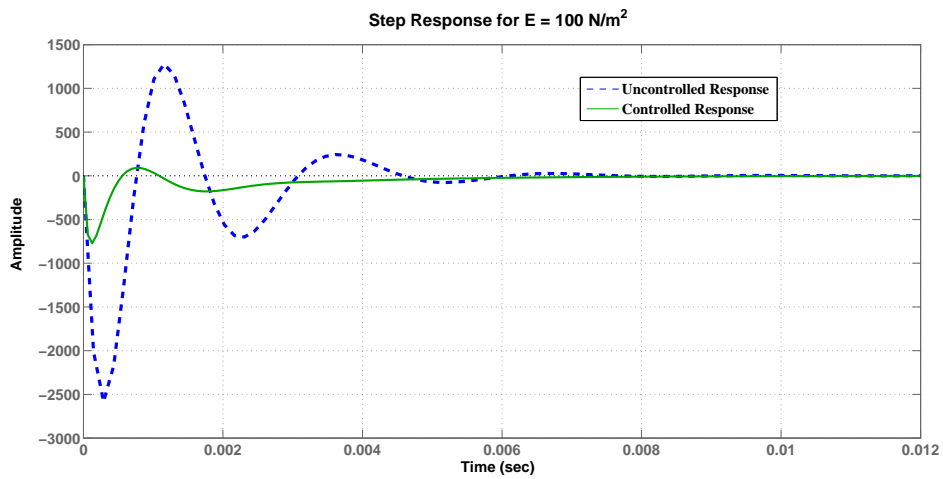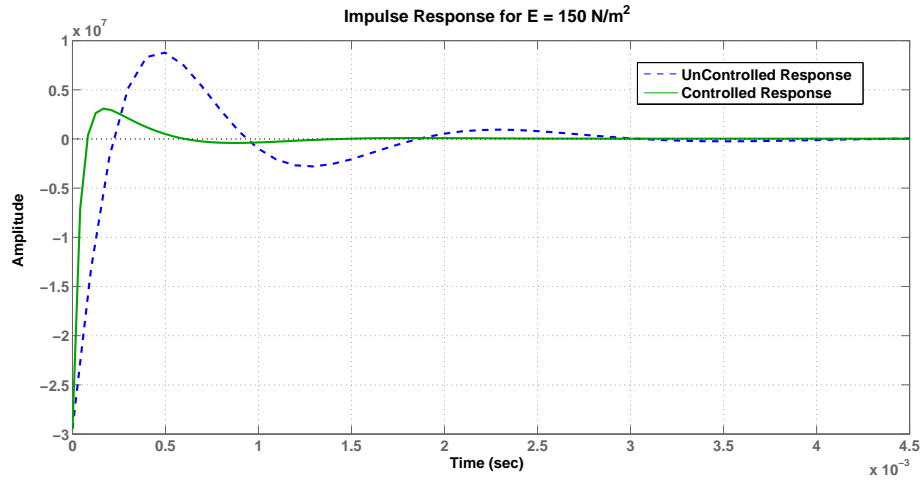
below for a step and impulse response.
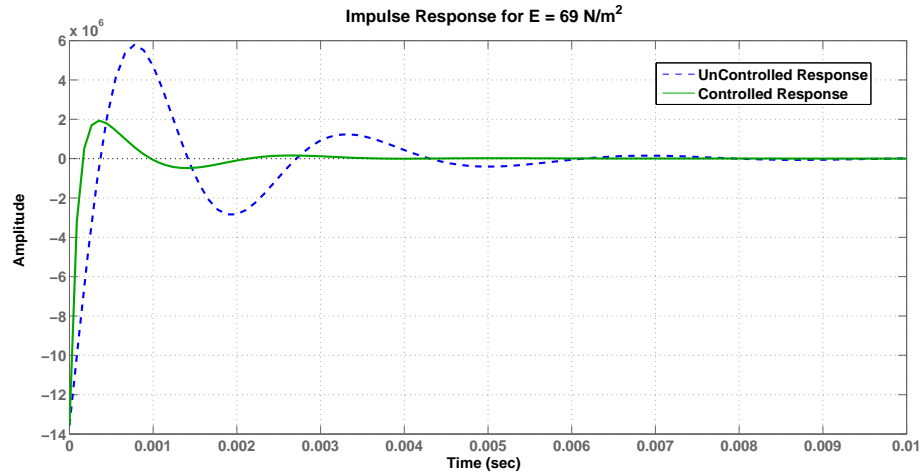
Figure 6.5: The figure shows the Impulse response for controlled and uncontrolled system at $E = 69N/m^2$
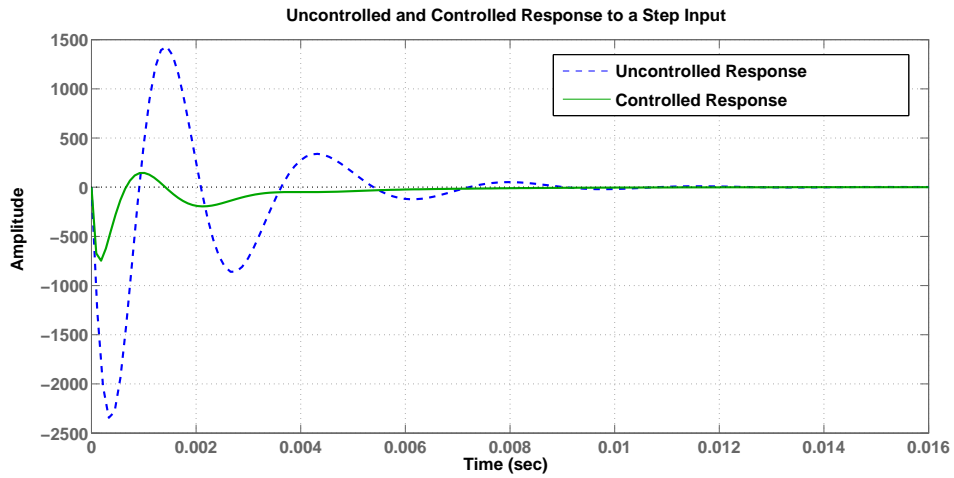


Figure 6.6: The figure shows the Step response for controlled and uncontrolled system at $E = 69N/m^2$

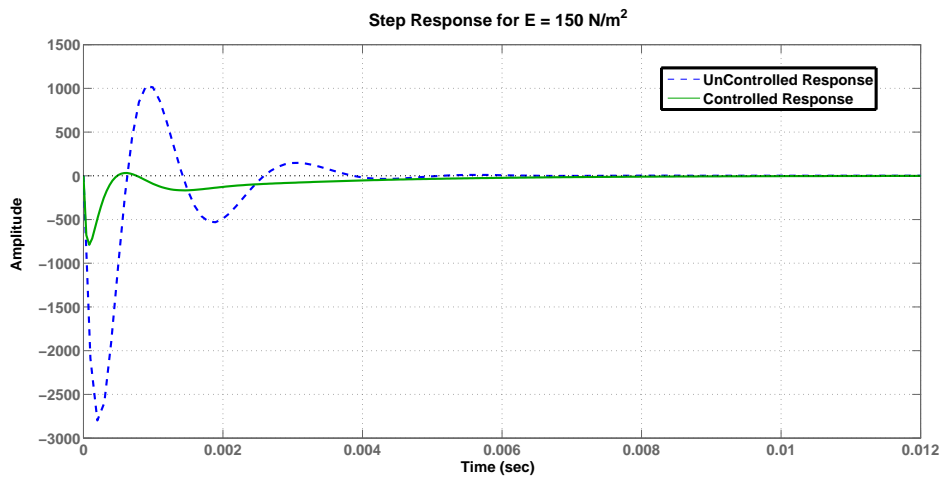Figure 6.7: The figure shows the Impulse response for controlled and uncontrolled system at $E = 100N/m^2$



Figure 6.8: The figure shows the Step response for controlled and uncontrolled system at $E = 100N/m^2$

Figure 6.9: The figure shows the Impulse response for controlled and uncontrolled system at $E = 150N/m^2$



Figure 6.10: The figure shows the Impulse response for controlled and uncontrolled system at $E = 150N/m^2$

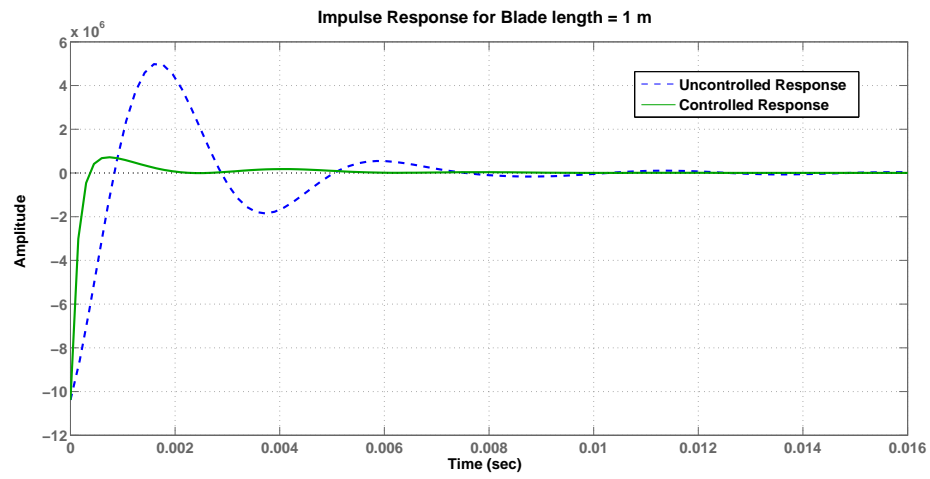## 6.7 The Effect of variation of Blade length



Figure 6.11: The figure shows the Impulse response for Blade Length of $1m$
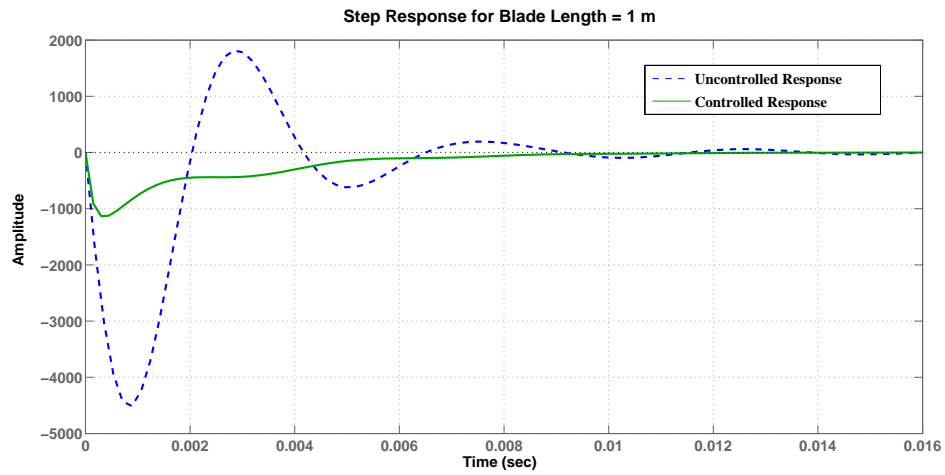


Figure 6.12: The figure shows the Step response for Blade Length of $1m$
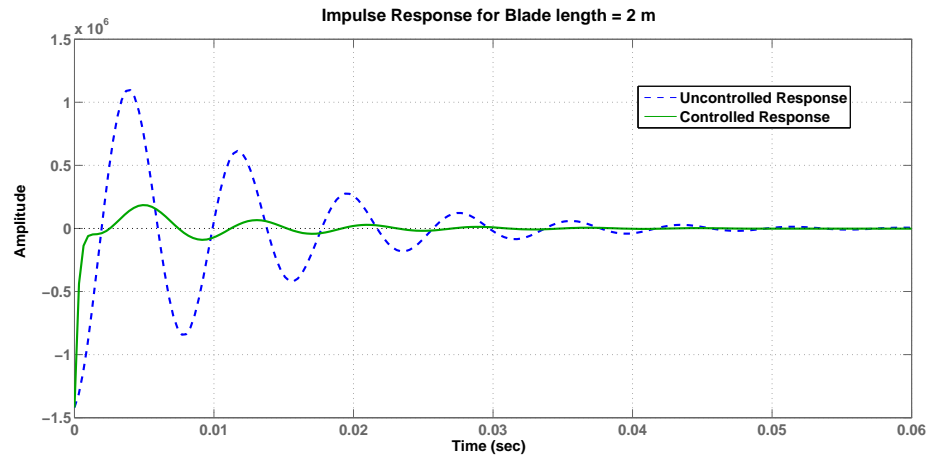
Figure 6.13: The figure shows the Impulse response for Blade Length of $2m$
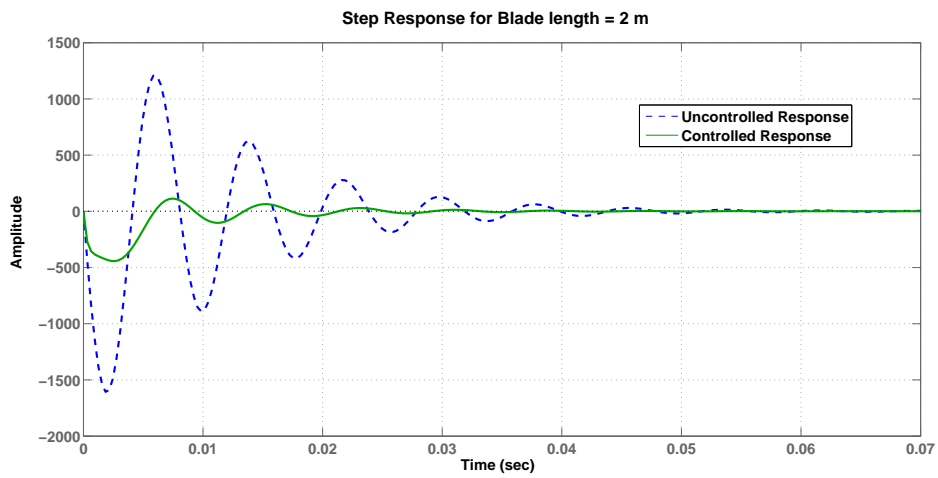


Figure 6.14: The figure shows the Step response for Blade Length of $2m$
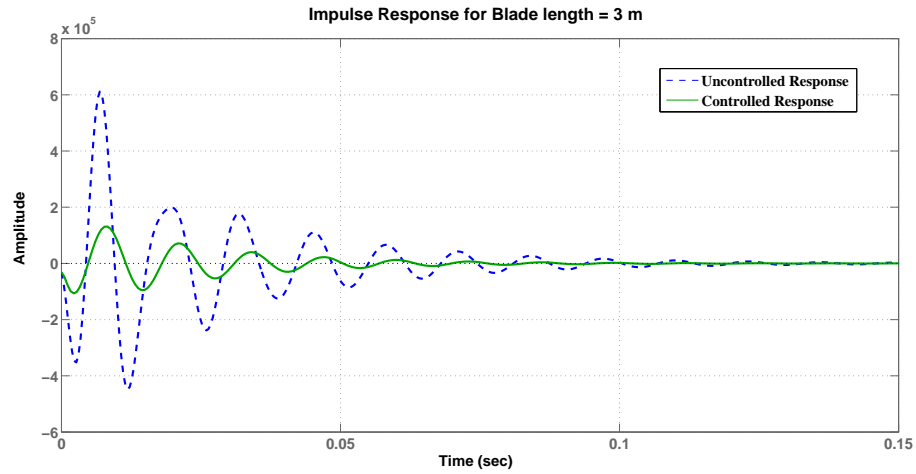
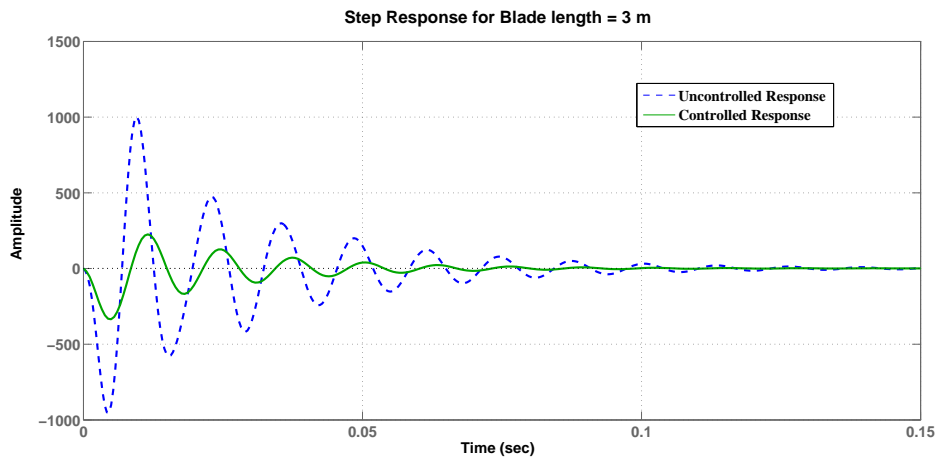Figure 6.15: The figure shows the Impulse response for Blade Length of $3m$



Figure 6.16: The figure shows the Step response for Blade Length of $3m$

# CHAPTER 7

# CONCLUSIONS

The work utilizes an innovative technique to obtain more accurate aeroelastic results which was previously only being used in suppressing helicopter vibrations. This allowed to simulate real time conditions and hence eventually contributed in the design of a more responsive controller. The following conclusions can be made from this study.

It can be noted from results that BEM model alone doesn't provide accurate results for the vibration model and the accuracy increased substantially under under varying dynamic conditions. The wind turbine aeroelastic model adopts a 3D formulation in a rotating frame of reference using finite element method. This formulation enables the overall aeroelastic model to account for mass distribution and allowed it to include elastic properties, geometric stiffness effects as well as account for dynamic conditions. The result from the aeroelastic models allow the evaluation of eigenvalues for finite element rotating beam solution. Thus, the LQR control strategies developed using this aeroelastic model is more responsive

and would accommodate for dynamic stall conditions. The results indicate that ONERA type model can be adopted after some modifications into the state space format. This aeroelastic model was used for suppression of edgewise vibrations in wind turbine blades.

# REFERENCES

[1] N. M. Wereley, G. Wang, and A. Chaudhuri, "Demonstration of Uniform Cantilevered Beam Bending Vibration Using a Pair of Piezoelectric Actuators," *Journal of Intelligent Material Systems and Structures*, vol. 22, no. 4, pp. 307–316, 2011. [Online]. Available: https://doi.org/10.1177/1045389X10379661

[2] P. I. Kattan, "The beam element," in *MATLAB Guide to Finite Elements: an Interactive Approach.* Springer, 2007, ch. 7.

[3] J. A. Karlsen, "Performance calculations for a model turbine," 2009.

[4] E. Logan Jr, *Handbook of turbomachinery.* CRC Press, 2003.

[5] J. Arrigan, V. Pakrashi, B. Basu, and S. Nagarajaiah, "Control of flapwise vibrations in wind turbine blades using semi-active tuned mass dampers," *Structural Control and Health Monitoring*, pp. 840–851, 2010. [Online]. Available: http://dx.doi.org/10.1002/stc.456

[6] J. F. Manwell, J. G. McGowan, and A. L. Rogers, "Aerodynamics of wind turbines," in *Wind energy explained: theory, design and application*. Wiley, 2002, ch. 3, pp. 83–138.

[7] R. Clark, D. Cox, J. Curtiss, H.C, J. W. Edwards, K. C. Hall, and D. A. Peters, *A Modern Course in Aeroelasticity*, E. H. DOWELL, Ed. KLUWER ACADEMIC PUBLISHERS, 2005.

[8] L. Chang, "Wind Energy Conversion Systems," *IEEE Canadian Review*, pp. 12–16, 2002. [Online]. Available: http://www.benthamdirect.org/pages/content.php?9781608052851

[9] "Statistical Bulletin 2016," Arab Union of Electricity, Tech. Rep. Issue 25, 2016.

[10] "Vision 2030," Kingdom of Saudi Arabia, Tech. Rep., 2016.

[11] S. El-Nakla, C. B. Yahya, H. Peterson, O. K. Ouda, and M. Ouda, "Renewable energy in saudi arabia: Current status, initiatives and challenges," in *IEEE - 2017 9th IEEE-GCC Conference and Exhibition (GCCCE)*. IEEE, May 2017, pp. 41–50.

[12] King Abdullah City for Atomic and Renewable energy. (2016) Wind Resources in Saudi Arabia. [Online]. Available: https://rratlas.kacare.gov.sa/RRMMPublicPortal/?q=en/Wind

[13] N. M. Al-Abbadi, "Wind energy resource assessment for five locations in saudi arabia," *Renewable Energy*, vol. 30,

no. 10, pp. 1489 – 1499, 2005. [Online]. Available: http://www.sciencedirect.com/science/article/pii/S0960148104004227

[14] A. A. W. E. Association, "AWEA Small Wind Turbine Global Market Study," Washington, DC, Tech. Rep., 2010.

[15] A. M. Eltamaly, "Design and implementation of wind energy system in saudi arabia," *Renewable Energy*, vol. 60, pp. 42 – 52, 2013. [Online]. Available: http://www.sciencedirect.com/science/article/pii/S0960148113002115

[16] R. Bianchi, F.D.; de battista, H.; Mantz, "The Wind and Wind Turbines," in *Wind Turbines Control System Principles , Modelling and Gain Scheduling design*, 1st ed. London, United Kingdom: Springer-Verlag London, 2007, ch. 2, pp. 7–28.

[17] D. Spera, "Introduction to modern wind turbines," in *Wind Turbine Technology: Fundamental Concepts in Wind Turbine Engineering*, 2nd ed. ASME, 2009, ch. 2, p. 47103.

[18] G. Genta, *Vibration dynamics and control*. Springer, 2009.

[19] T. J. Larsen, A. M. Hansen, and T. Buhl, "Aeroelastic effects of large blade deflections for wind turbines," in *Proceedings of the Special Topic Conference The Science of Making Torque From Wind*, 2004, pp. 238–246.

[20] N. R. Council *et al.*, *Assessment of research needs for wind turbine rotor materials technology*. National Academies Press, 1991.

[21] E. A. Bossanyi, "Individual blade pitch control for load reduction," *Wind Energy*, vol. 6, no. 2, pp. 119–128, 2003.

[22] Y.-c. Fung, "Engineering flutter analysis and structural design," in *An Introduction to the Theory of Aeroelasticity*, 1st ed. Dover, 1993, ch. 7, pp. 246–271.

[23] M. M. Hand, *Mitigation of wind turbine/vortex interaction using disturbance accommodating control*. National Renewable Energy Laboratory Boulder, CO, 2003.

[24] S. J. Johnson, C. P. C. V. Dam, and D. E. Berg, "Active Load Control Techniques for Wind Turbines," Livermore, California, Tech. Rep. August, 2008. [Online]. Available: http://www.osti.gov/bridge/product.biblio.jsp?osti_id=943932

[25] P. Andre, *Vibration Control of Active Structures: An Introduction*. Springer, 2011.

[26] N. Jalili, "Vibration Control Using Piezoelectric Actuators and Sensors Contents," in *Piezoelectric-Based Vibration Control: From Macro to Micro/Nano Scale Systems*, 1st ed. Springer Science + Business Media LLC, 2010, ch. 9, pp. 233–306.

[27] R. Vepa, *Dynamics of smart structures*. John Wiley & Sons, 2010.

[28] M. N. Svendsen, "Wind Turbine Rotors with Active Vibration Control," PhD Thesis, Technical University of Denmark, Denmark, 2011.

[29] A. Bazoune and Y. A. Khulief, "A finite beam element for vibration analysis of rotating tapered timoshenko teams," *Journal of Sound and Vibration*, vol. 156, no. 1, pp. 141–164, 1992.

[30] Y. Khulief, "Vibration suppression in using active modal control," *Journal of sound and vibration*, vol. 242, no. 4, pp. 681–699, 2001.

[31] Baillargeon, Brian P., "Active Vibration Suppression of Smart Structures Using Piezoelectric Shear Actuators," 2003.

[32] J. B. Gunda, A. P. Singh, P. S. Chhabra, and R. Ganguli, "Free Vibration Analysis of Rotating Tapered Blades using Fourier-p Superelement," *Structural Engineering and Mechanics*, vol. 27, no. 2, pp. 243–257, 2007.

[33] J. G. Leishman, "Principles of helicopter aerodynamics." Cambridge University Press, 2006, ch. 7. Aerodynamics of Rotor Airfoil, pp. 347–416.

[34] J. W. Larsen, S. R. K. Nielsen, and S. Krenk, "Dynamic stall model for wind turbine airfoils," *Journal of Fluids and Structures*, vol. 23, no. 7, pp. 959–982, 2007.

[35] J. G. Leishman and T. S. Beddoes, "A semi-empirical model for dynamic stall," vol. 34, pp. 3–17, 1989.

[36] M. H. Hansen, M. Gaunaa, and H. a. Madsen, "A Beddoes-Leishman type dynamic stall model in state-space and indicial formulations," Roskilde, Denmark, Tech. Rep. Ris{ø}-R-1354(EN), 2004. [Online]. Available: http://www.risoe.dk/rispubl/vea/veapdf/ris-r-1354.pdf

[37] A. Nour, M. T. Gherbi, and Y. Chevalier, "Modes shape and harmonic analysis of different structures for helicopter blade," *30th European Conference on Acoustic Emission Testing & 7th International Conference on Acoustic Emission University of Granada*, no. September, pp. 12–15, 2012.

[38] L. Liu, "BVI Induced Vibration and Noise Alleviation," PhD Thesis, University of Michigan, 2005.

[39] S. Krenk, M. Svendsen, and J. Hogsberg, "Resonant vibration control of three-bladed wind turbine rotors," vol. 50, no. 1, 2012.

[40] N. Li and M. J. Balas, "Aeroelastic Vibration Suppression of a Rotating Wind," in *32nd ASME Wind Energy Symposium*, no. January. National Harbor, Maryland: American Institute of Aeronautics and Astronautics, 2014, pp. 1–9.

[41] M. Roura, A. Cuerva, A. Sanz-Andres, and A. Barrero-Gill, "A panel method free-wake code for aeroelastic rotor predictions," *Wind Energy*, pp. 357–371, 2009. [Online]. Available: http://onlinelibrary.wiley.com/doi/10.1002/we.1608/full

[42] M.-S. Jeong, S.-J. Yoo, and I. Lee, "Aeroelastic Analysis for Large Wind Turbine Rotor Blades," in *52nd AIAA/ASME/ASCE/AHS/ASC Structures, Structural Dynamics and Materials Conference*, no. April. Denver, Colorado: American Institute of Aeronautics and Astronautics, 2011, pp. 1–7.

[43] F. Zou, V. a. Riziotis, S. G. Voutsinas, and J. Wang, "Analysis of vortex-induced vibrations using a free-wake aero-elastic tool," *Wind Energy*, vol. 18, no. 12, pp. 2145–2169, 2013.

[44] W. Skrzypinski, "Analysis and Modeling of Unsteady Aerodynamics with Application to Wind Turbine Blade Vibration at Standstill Conditions," PhD Thesis, Technical University of Denmark, 2012.

[45] Y. Bichiou, A. Abdelkefi, and M. Hajj, "Nonlinear Aeroelastic Characterization of Wind Turbine Blades," in *Journal of Vibration and Control*, no. April. Blacksburg, Virginia: American Institute of Aeronautics and Astronautics, 2014, pp. 1–10. [Online]. Available: http://jvc.sagepub.com/cgi/doi/10.1177/1077546314529986

[46] L. Wenzhi and W. Jianxin, "3D Modeling Methods of Aerodynamic Shape for Large-Scale Wind Turbine Blades," in *International Conference on Information Technology and Computer Science*. Islamabad: IEEE computer society, 2009, pp. 7–10.

[47] A. Staino, B. Basu, and S. R. K. Nielsen, "Actuator control of edgewise vibrations in wind turbine blades," *Journal of Sound and Vibration*, vol. 331, no. 6, pp. 1233–1256, 2012. [Online]. Available: http://dx.doi.org/10.1016/j.jsv.2011.11.003

[48] L. O. Bernhammer and R. De Breuker, "Wind Turbine Structural Model Using Non-Linear Modal Formulations," in *32nd ASME Wind Energy Sym-*

*posium*, no. January. National Harbor, Maryland: American Institute of Aeronautics and Astronautics, 2014, pp. AIAA 2014–0715.

[49] L. Bernhammer, R. De Breuker, van Kuik, and G.A.M., "DU-SWAT: A New Aeroelastic Horizontal Axis Wind Turbine Analysis Tool," in *8th Phd Seminar on Wind Energy in Europe*, no. September. Zurich, Switzerland: European Academy of Wind Enegry (EAWE), 2012.

[50] S. Alpay, A. Barut, and E. Madenci, "An efficient modeling approach for dynamic simulation of wind turbine blades," *Aiaa*, vol. 2739, no. April, pp. 1–11, 2010. [Online]. Available: http://www.aric.or.kr/treatise/journal/content.asp?idx=126712

[51] D. A. Peters, D. Barwey, and A. Su, "An integrated airloads-inflow model for use in rotor aeroelasticity and control analysis," *Mathematical and computer modelling*, vol. 19, no. 3-4, pp. 109–123, 1994.

[52] N. Li and M. J. Balas, "Flutter Suppression of Rotating Wind Turbine Blade Based on Beddoes-Leishman model using Microtabs," in *AIAA Modeling and Simulation Technologies (MST) Conference*. Boston, MA: American Institute of Aeronautics and Astronautics, 2013, pp. 1–12.

[53] Q. Wang, M. A. Sprague, J. Jonkman, and N. Johnson, "Nonlinear Legendre Spectral Finite Elements for Wind Turbine Blade Dynamics," in *32nd ASME Wind Energy Symposium*, no. January. National Harbor, Maryland: American Institute of Aeronautics and Astronautics, 2014, pp. 1–13.

[54] P. Couturier, S. Krenk, and P. J. Couturier, "Efficient Beam-Type Structural Modeling of Rotor Blades," in *Proceedings of the EWEA Annual Event and Exhibition.* European Wind Energy Association (EWEA), 2015, pp. 1–8.

[55] A. Kumar, A. Dwivedi, V. Paliwal, and P. P. Patil, "Free Vibration Analysis of Al 2024 Wind Turbine Blade Designed for Uttarakhand Region Based on FEA," in *48th AIAA Aerospace Sciences Meeting Including the New Horizons Forum and Aerospace Exposition.* Dehradun, Uttarakhand: 2nd International Conference on Innovations in Automation and Mechatronics Engineering, ICIAME, 2014.

[56] K. L. Van Buren, M. G. Mollineaux, and F. M. Hemez, "Simulating the dynamics of wind turbine blades: Part I, model development and verification," in *52nd AIAA/ASME/ASCE/AHS/ASC Structures, Structural Dynamics and Materials Conference.* Denver, Colorado: American Institute of Aeronautics and Astronautics, 2011.

[57] K. L. V. Buren, M. G. Mollineaux, and F. M. Hemez, "Simulating the Dynamics of Wind Turbine Blades : Part II , Model Validation and Uncertainty Quantification," in *52nd AIAA/ASME/ASCE/AHS/ASC Structures, Structural Dynamics and Materials Conference*, no. April. Denver, Colorado: American Institute of Aeronautics and Astronautics, 2011, pp. 1–18.

[58] A. Y. T. Leung, "Vibration of thin pre-twisted helical beams," *International Journal of Solids and Structures*, vol. 47, no. 9, pp. 1177–1195, 2010.

[59] D. Garinis, M. Dinulović, and B. Rašuo, "Dynamic analysis of modified composite helicopter blade," *FME Transactions*, vol. 40, no. 2, pp. 63–68, 2012.

[60] K. L. V. Buren, M. G. Mollineaux, F. M. Hemez, and D. Luscher, "Developing Simplified Models for Wind Turbine Blades," in *14th AIAA Non-Deterministic Approaches Conference*, no. April.  Honolulu, Hawaii: American Institute of Aeronautics and Astronautics, 2012, pp. 1–15.

[61] Y. A. Khulief, "Active modal control of vibrations in elastic structures in the presence of material damping," *Computer Methods in Applied Mechanics and Engineering*, vol. 190, no. 51-52, pp. 6947–6961, 2001.

[62] J. Fei, Y. Fang, and C. Yan, "The Comparative study of vibration control of flexible structure using smart materials," *Mathematical Problems in Engineering*, vol. 2010, p. 13, 2010.

[63] M. A. Rotea, M. A. Lackner, and R. Saheba, "Active Structural Control of Offshore Wind turbines," in *48th AIAA Aerospace Sciences Meeting Including the New Horizons Forum and Aerospace Exposition*, no. January.  Orlando, Florida: American Institute of Aeronautics and Astronautics, 2010, pp. 1–21.

[64] S. F. Ali and R. Padhi, "Active vibration suppression of nonlinear beams using optimal dynamic inversion," *Proceedings of the Institution of Mechanical Engineers, Part I: Journal of Systems and Control Engineering*, vol. 223, no. 5, pp. 657–672, 2009. [Online]. Available: http://pii.sagepub.com/lookup/doi/10.1243/09596518JSCE688

[65] Z. Zhang, "Wind Turbine Vibration Study : A Data Driven Methodology," 2009.

[66] C. Bai, F. Hsiao, M. Li, G. Huang, and Y. Chen, "Design of 10 kw horizontal-axis wind turbine (hawt) blade and aerodynamic investigation using numerical simulation," *Procedia Engineering*, vol. 67, pp. 279–287, 2013.

[67] I. Farzad, "Transverse vibration analysis of analytical approximate techniques euler-bernoulli beams using analytical approximate techniques," in *Advances in Vibration Analysis Research*, 1st ed.  InTech, 2011, ch. 1, pp. 1–22.

[68] M. Geradin and D. Rixen, *Mechanical Vibrations: Theory and Application to Structural Dynamics*.  Wiley, 2015.

[69] M. Svendsen, S. Krenk, and J. Hgsberg, "Resonant vibration control of wind turbine blades," in *TORQUE 2010*, 2010, pp. 543–553.

[70] S. Krenk and P. J. Couturier, "Equilibrium-based nonhomogeneous anisotropic beam element," *AIAA Journal*, 2017.

[71] S. Ilanko, L. E. Monterrubio, and Y. Mochida, "The rayleigh-ritz method and simple applications," in *The Rayleigh-Ritz Method for Structural Analysis*, 1st ed.  ISTE Ltd and John Wiley & Sons, Inc., 2014, ch. 3, pp. 21–31.

[72] S. S. Rao, "Dynamic analysis," in *The Finite Element Method in Engineering*, 4th ed., 2009, ch. 12, p. 429.

# Vitae

- **Name** :        Hamza Ahmed Mir

- **Nationality**:      Pakistani

- **Date of Birth**:    26/06/1989

- **Email**:          *hamza.ahmed.mir@outlook.com*

- **Permenant Address**: House # 60, Lane # 02, Street # 03, Mukarram Town, Rawalpindi 46000, Pakistan

- **Academic Background**:

  BSc Aerospace Engineering (Institute of Space Technology)

- **Research Interests**: Vibration Control, Aeroelasticity, Dynamic Modeling

- **Awards**:

  1. First Rank in KFUPM 8th Student Forum, 2017

  2. Second Rank in KFUPM 9th Student Forum, 2018

**Journal Publications**:

  1. Mir, H.A., Abdelrahman, W.G. "Vibration Control of Wind Turbines Blades Edgewise Vibrations using LQR," 2018.

  2. Mir, H.A., Abdelrahman, W.G. "A Comparative Study of Aeroelastic Models for Actively Controlled Smart Wind Turbines Blades," 2018.